Atmospheric
Chemistry
and Physics
Discussions

Open Access

Projected effect of 2000–2050 changes in climate and emissions on aerosol levels in China and associated transboundary transport

H. Jiang[1,2], H. Liao[1], H. O. T. Pye[3], S. Wu[4], L. J. Mickley[5], J. H. Seinfeld[6], and X. Zhang[7]

[1]State Key Laboratory of Atmospheric Boundary Layer Physics and Atmospheric Chemistry (LAPC), Institute of Atmospheric Physics, Chinese Academy of Sciences, Beijing, China
[2]Graduate University of Chinese Academy of Sciences, Beijing, China
[3]National Exposure Research Laboratory, Environmental Protection Agency, Research Triangle Park, North Carolina, USA
[4]Department of Geological and Mining Engineering and Sciences and Department of Civil and Environmental Engineering, Michigan Technological University, Houghton, Michigan, USA
[5]School of Engineering and Applied Sciences, Harvard University, Cambridge, Massachusetts, USA
[6]Departments of Chemical Engineering and Environmental Science and Engineering, California Institute of Technology, Pasadena, California, USA

ACPD

13, 6501–6551, 2013

Projected 2000–2050 changes in aerosols in China

H. Jiang et al.

Title Page

Abstract | Introduction

Conclusions | References

Tables | Figures

◄◄ | ►►

◄ | ►

Back | Close

Full Screen / Esc

Printer-friendly Version

Interactive Discussion

[7]Key Laboratory for Atmospheric Chemistry, Chinese Academy of Meteorological Sciences, CMA, Beijing, China

Correspondence to: H. Liao (hongliao@mail.iap.ac.cn)

Projected 2000–2050 changes in aerosols in China

H. Jiang et al.

Title Page

Abstract	Introduction
Conclusions	References
Tables	Figures

Back | Close

Full Screen / Esc

Printer-friendly Version

Interactive Discussion

Abstract

We investigate the 2000–2050 changes in concentrations of aerosols in China and the associated transboundary aerosol transport by using the chemical transport model GEOS-Chem driven by the Goddard Institute for Space Studies (GISS) general circulation model (GCM) 3 at $4° \times 5°$ resolution. Future changes in climate and emissions projected by the IPCC A1B scenario are imposed separately and together through sensitivity simulations. Accounting for sulfate, nitrate, ammonium, black carbon (BC), and organic carbon (OC) aerosols, concentrations of individual aerosol species change by -2.3 to $+1.7 \, \mu g \, m^{-3}$ and $PM_{2.5}$ levels are projected to change by about 10–20 % in eastern China as a result of 2000–2050 change in climate alone. With future changes in anthropogenic emissions alone, concentrations of sulfate, BC, and OC are simulated to decrease because of reductions in emissions, and those of nitrate are predicted to increase because of higher NO_x emissions combined with decreases in sulfate. The net result is a reduction of seasonal mean $PM_{2.5}$ concentrations in eastern China by $2–9.5 \, \mu g \, m^{-3}$ (or 10–30 %) over 2000–2050. It is noted that current emission inventories for BC and OC over China are found to be inadequate at present. Transboundary fluxes of different aerosol species show different sensitivities to future changes in climate and emissions. The annual outflow of $PM_{2.5}$ from eastern China to the western Pacific is estimated to change by -6.0 %, -1.5 %, and -9.0 % over 2000–2050 owing to climate change alone, changes in emissions alone, and changes in both climate and emissions, respectively. The fluxes of nitrate and ammonium aerosols from Europe and Central Asia into western China increase over 2000–2050 by changes in emissions, leading to a 15 % increase in annual inflow of $PM_{2.5}$ to western China with future changes in both emissions and climate. Fluxes of BC and OC from South Asia to China in spring contribute to a large fraction of the annual inflow of $PM_{2.5}$. The annual inflow of $PM_{2.5}$ from South Asia and Southeast Asia to China is estimated to change by -55 %, $+133$ %, and $+63$ % over 2000–2050 owing to climate change alone, changes in emissions alone, and changes in both climate and emissions, respectively. While the

Title Page

Abstract | Introduction

Conclusions | References

Tables | Figures

|◀ | ▶|

◀ | ▶

Back | Close

Full Screen / Esc

Printer-friendly Version

Interactive Discussion

$4° \times 5°$ spatial resolution is a limitation of the present study, the direction of predicted changes in aerosol levels and transboundary fluxes still provides valuable insight into future air quality.

1 Introduction

Aerosols are important air pollutants that lead to negative health impacts, reductions in visibility, and changes in climate (Intergovernmental Panel on Climate Change (IPCC), 2007). Concentrations of major atmospheric aerosol species, sulfate, nitrate, ammonium, black carbon, organic carbon, and mineral dust, are especially high in China (Matsui et al., 2009; Tie and Cao, 2010; Qu et al., 2010; Cao et al., 2012), driven by a combination of direct and precursor emissions (Streets et al., 2003) and regional meteorological conditions (Zhang et al., 2010a; Zhu et al., 2012). Estimating future aerosol levels in China is essential in considerations of air quality both over China itself and in the Northern Hemisphere.

In the absence of changes in emissions of primary aerosols as well as aerosol precursors, climate change itself will influence future aerosol levels. For example, coupled climate–chemical transport modeling studies show that climate change alone can lead to increased surface ozone in anthropogenically impacted regions by 1–10 ppbv in summertime over the coming decades, based on the IPCC future scenarios (Jacob and Winner, 2009). This increase is a result of slower transport, enhanced biogenic hydrocarbon emissions, and accelerated decomposition of peroxyacetyl nitrate (PAN) at higher temperatures (Hogrefe et al., 2004; Liao et al., 2006; Murazaki and Hess, 2006; Steiner et al., 2006; Racherla and Adams, 2008; Wu et al., 2008; Jacob and Winner, 2009; Andersson and Engardt, 2010; Chang et al., 2010; Lam et al., 2011; Katragkou et al., 2011; Langner et al., 2012; Reuten et al., 2012; Wang et al., 2013). A warmer future climate is also predicted to influence aerosol levels over the United States and Europe by as much as $1 \mu g m^{-3}$ through altered concentrations of atmospheric oxidants, by changed precipitation and boundary layer height, and by shifting gas-particle

equilibria (Liao et al., 2006; Unger et al., 2006; Bauer et al., 2007; Jacob and Winner, 2009; Pye et al., 2009; Day and Pandis, 2011; Lam et al., 2011; Tai et al., 2012, 2013; Juda-Rezler et al., 2012). Because of the enormous importance of China as a source of aerosols, a study that addresses how aerosol levels in China may change over the coming decades is called for.

Another issue that is associated with the aerosol levels in China is the future transboundary aerosol transport. A number of observational and modeling analyses have demonstrated the importance of present-day long-range transport of aerosols from East Asia. Surface observations at island sites (Huebert et al., 2001; Prospero et al., 2003) and aircraft observations in Asian outflow over the Northwest Pacific (Jordan et al., 2003; Maxwell-Meier et al., 2004) and the Northeast Pacific (Clarke et al., 2001; Price et al., 2003) have documented the spring maximum in transpacific transport. By using the global atmospheric chemical transport model GEOS-Chem, Park et al. (2003) predicted that transpacific transport contributed to about 10 % of the annual mean natural background surface-layer concentrations of black carbon over the United States. By using satellite measurements of aerosol optical depth over the North Pacific together with GEOS-Chem simulation, Heald et al. (2006) showed that transport from Asia led to a seasonal mean increase of surface-layer sulfate concentration of 0.16 $\mu g\,m^{-3}$ (with 50 % uncertainty) in the northwestern United States in spring of 2001. Chin et al. (2007) predicted an enhancement of similar magnitude in surface-layer sulfate aerosol in the western United States in 2001 by long-range aerosol transport; the annual mean contribution to sulfate concentration was estimated to be 0.1–0.2 $\mu g\,m^{-3}$ using the global model GOCART. Yu et al. (2008) performed a satellite-based assessment of transpacific transport of anthropogenic and biomass burning aerosols based on years 2002–2005 aerosol optical depths from the Moderate Resolution Imaging Spectroradiometer (MODIS). They estimated that about 25 % of aerosol mass exported from East Asia to the northwestern Pacific Ocean can reach the west coast of North America. Two studies examined aerosol transport from Europe and South Asia to China. Chin et al. (2007) estimated that European emissions can increase the surface ammonium

sulfate concentrations over eastern Asia by 0.2–0.5 µg m^{-3}. Using the GEOS-Chem model, Zhang et al. (2010b) estimated that organic carbon aerosol from South Asia contributed 50–70 % of OC mass over southern China and 20–50 % of OC over the western North Pacific in the middle troposphere in summer of 1998.

We present here a study to estimate: (1) the changes of aerosol levels in China over the years 2000–2050 as a result of projected changes in emissions and climate, (2) the changes of transboundary fluxes of aerosols into or out of China over this time period. This study builds on two previous ones. Liao et al. (2007) used the Goddard Institute for Space Studies (GISS) general circulation model (GCM) 3 to drive GEOS-Chem to simulate climatological present-day aerosol levels in the United States, and Pye et al. (2009) investigated the effects of projected climate and emissions changes on 2000–2050 sulfate-nitrate-ammonium aerosols in the United States using the same GISS Model 3/GEOS-Chem combination. As a basis for the present study, the IPCC emission scenario A1B (Nakicenovic and Swart, 2000) is adopted; this scenario represents a future world with rapid economic growth and introduction of new and more energy-efficient technologies. GISS Model 3 global meteorological fields are used to drive the atmospheric chemical transport model GEOS-Chem for both present day (1999–2001) and years 2049–2050. Effects of climate change alone, emission changes alone, and both climate and emissions changes on aerosol levels and transboundary fluxes are simulated. The models in present study have a relatively coarse spatial resolution of 4° latitude by 5° longitude, which are not expected to capture the characteristically high concentrations of aerosols in China's major urban areas. Nevertheless, the direction of projected changes in aerosol levels should be correctly predicted.

The methods and model setup used to simulate present-day and year 2050 aerosols are described in Sect. 2. Section 3 evaluates simulated present-day concentrations of aerosols in China. Section 4 shows predictions of future aerosol levels over China due to changes in climate alone, emissions alone, and combined climate and emissions changes, and Sect. 5 estimates future changes in transboundary transport of aerosols to examine inflow to and outflow from China.

2 Methods

2.1 GEOS-Chem/GISS models

The atmospheric chemical transport model, GEOS-Chem (v.7-4-11, http://acmg.seas.harvard.edu/geos/) is driven by the GISS Model 3 meteorological data (Rind et al., 2007). Both the GISS Model 3 and the GEOS-Chem models have a horizontal resolution of 4° latitude by 5° longitude with 23 vertical layers. The interface between GEOS-Chem and the GISS meteorological fields is described by Wu et al. (2007) and Pye et al. (2009), and the same meteorology from the work of Wu et al. (2008) is used here. The GEOS-Chem model includes coupled ozone-NO_x-hydrocarbon (~ 80 species, ~ 300 chemical reactions) (Bey et al., 2001) and aerosol chemistry. Aerosol species simulated in the GEOS-Chem model include sulfate (SO_4^{2-})/nitrate (NO_3^-)/ammonium (NH_4^+) (Park et al., 2004; Pye et al., 2009), primary organic carbon (OC) and black carbon (BC) (Park et al., 2003), secondary organic aerosol (SOA), sea salt (Alexander et al., 2005), and mineral dust (Fairlie et al., 2007). SOA formation considers the oxidation of isoprene (Henze and Seinfeld, 2006), monoterpenes and other reactive VOCs (ORVOCs) (Liao et al., 2007), and aromatics (Henze et al., 2008). We are focused on future changes in anthropogenic aerosols in this work; the assessment on mineral dust and sea salt aerosols will be our future work.

2.2 Emissions

Present-day and year 2050 assumed anthropogenic emissions of aerosol precursor and aerosols are listed in Table 1. Emissions of O_3 precursors (including NO_x, CO, and nonmethane VOCs) follow those in Wu et al. (2008), and those of NH_3 and SO_2 are taken from Pye et al. (2009). The base year for present-day anthropogenic emissions is 1999 for the United States (Wu et al., 2008) and 1998 elsewhere (Pye et al., 2009). Year 2050 anthropogenic emissions of ozone precursors, aerosol precursors, and aerosols from the IPCC A1B scenario were generated by the Integrated Model to Assess the

Greenhouse Effect (IMAGE) socioeconomic model using prescribed growth factors for different regions, species, and sources (Streets et al., 2004). Ammonia emissions have an imposed seasonality that was determined as a function of temperature for one base year in this model. In present day, anthropogenic emissions of NO_x, CO, NMVOCs,

5   SO_2, NH_3, OC, and BC in eastern China are estimated to account for 12 %, 16 %, 12 %, 20 %, 18 %, 10 %, and 19 %, respectively, of the total global emissions. Relative to the assumed present day, year 2050 anthropogenic emissions of NO_x, CO, NMVOCs, SO_2, NH_3, OC, and BC in eastern China (20–55° N, 98–125° E) are estimated to change by +72 %, −7 %, +86 %, −29 %, −12 %, −40 %, and −59 %, respectively.

10   Present-day and year 2050 natural emissions of ozone and aerosol precursors include NO_x from lightning and soil, and biogenic hydrocarbons (Table 2), which are calculated based on the GISS Model 3 meteorological parameters. Lightning NO_x emissions are parameterized based on convective cloud-top height (Price and Rind, 1992; Wang et al., 1998). Soil NO_x emissions are calculated as a function of temper-

15   ature, wind speed, and precipitation (Yienger and Levy, 1995). Representation of biogenic emissions follows the algorithm of Guenther et al. (1995), which considers light and temperature dependence but does not account for the suppression of isoprene emissions under elevated ambient CO_2 concentrations (Rosenstiel et al., 2003) and climate-induced changes in land-cover. Simulated natural emissions of NO_x and bio-

20   genic hydrocarbons in eastern China are estimated to increase, respectively, by +20 % and +21 % over 2000–2050, with the increases in biogenic emissions resulting mainly from the future increases in temperature.

2.3   Projected climate change in China over 2000–2050

Present-day meteorological conditions from the NASA GISS Model 3 were simulated

25   with greenhouse gas levels corresponding to years 1999–2001. Year 2049–2051 climate was obtained from a simulation in which CO_2 and other greenhouse gases follow the IPCC A1B scenario. Note that the direct and indirect effects of aerosols are not considered in the simulation of 2000–2050 climate change. We have compared the

GISS Model 3 predictions of present-day (1999–2001) temperature, wind, and precipitation with assimilated meteorological parameters for 1999–2001 from the Godard Earth Observing System (GEOS)-4 of the NASA Global Modeling and Assimilation Office (GMAO) (http://acmg.seas.harvard.edu/geos/geos_sim.html). The GISS model captures fairly well the pattern and magnitude of surface air temperatures and zonal winds in China. The present-day precipitation simulated by the GISS model shows larger values in MAM and JJA than in DJF and SON, which agree with the assimilated precipitation, but the model overestimates precipitation in the middle and lower reaches of the Yangtze River in MAM whereas underestimates precipitation in that region in JJA.

Figure 1 shows the projected changes in surface air temperature in China from present day to year 2050 by long-lived greenhouse gases under the IPCC A1B scenario. Over the period 2000–2050, surface air temperatures in December-January-February (DJF) and March-April-May (MAM) are estimated to increase by up to 2 K in eastern China and exceed 2 K in western China, with the strongest warming of 3–4 K downwind of the Tibetan Plateau in DJF. In June-July-August (JJA) and September-October-November (SON), surface air temperatures are estimated to generally increase by 1–2 K throughout China, except those in some areas of southern, northeastern, and western China, which exhibit warming of 2–3 K. Warming under scenario A1B is generally predicted to be more pronounced than under scenario B1 and less pronounced than under A2 (IPCC, 2007).

Projected changes in precipitation in China from present day to year 2050 are shown in Fig. 2. Relative to present-day, year 2050 precipitation in DJF is estimated to nearly double in northern China and decrease by about 20–40 % in southern China; note that the present-day precipitation in DJF is the smallest among all seasons. In MAM, year 2050 precipitation is estimated to increase by about 20 % in southern China where the present-day seasonal precipitation is greatest. Precipitation is predicted to generally increase in eastern China in JJA and SON, reflecting mainly changes in convective precipitation. Note that the projected patterns of precipitation changes (the increases in precipitation in northern China in DJF and the increases in precipitation

in eastern China in JJA) from the GISS Model 3 generally agree with those from the IPCC AR4 multi-model predictions for China under the A1B scenario (IPCC, 2007). Projected changes in cloud fraction in China from present day to year 2050 are shown in Fig. 3. Changes in cloud fraction correspond well with the changes in precipitation; decreases (or increases) in clouds are associated with the decreases (or increases) in precipitation (Fig. 2).

The projected changes in the planetary boundary layer (PBL) depth in China between present-day and 2050 are shown in Fig. 4. In a warmer 2050, the PBL depths over the heavily populated eastern China are predicted to generally decrease in MAM and SON. Reductions in PBL depth are also predicted in northern China in DJF and in southern China in JJA. Simulated changes in the seasonal mean PBL depth in China are in the range of −15 % to +20 %. The changes in PBL depth result from the simulated changes in atmospheric temperature (or atmospheric stability); a more unstable atmosphere leads to higher PBL depths.

2.4   Simulations

We perform simulations for four cases: (1) year 2000 climate and emissions, (2) 2050 climate and 2000 anthropogenic emissions of aerosol precursor and aerosols, (3) 2000 climate and 2050 anthropogenic emissions of aerosol precursor and aerosols, and (4) 2050 climate and emissions. Each case is integrated for 3 yr (1999–2001 or 2049–2051) following 1 yr of model spin-up. All the results presented in this paper are 3-yr averages.

3   Simulated present-day O_3 and aerosols

3.1   Ozone

Figure 5 shows the simulated 1999–2001 seasonal surface-layer concentrations of O_3. The O_3 concentrations of 50–60 ppbv over the Tibet Plateau in MAM are a result of

stratospheric intrusion (Wild and Akimoto, 2001). As expected, concentrations of O_3 are the highest in JJA, with the values of 40–72 ppbv in eastern China. These simulated concentrations in JJA agree in magnitude with the observations in a number of urban and mountain sites in eastern China, as shown in the studies of Wang et al. (2001), Li et al. (2007), and Wang et al. (2008).

3.2 Aerosols

Figure 5 shows simulated 1999–2001 seasonal mean concentrations of SO_4^{2-}, NO_3^-, NH_4^+, BC, OC, and $PM_{2.5}$ (sum of SO_4^{2-}, NO_3^-, NH_4^+, BC, and OC) in China. Sulfate exhibits maximum concentrations of 3–7 µg m^{-3} in DJF and SON, which result from the net effect of production via photochemistry and removal by wet deposition. Although strong photochemistry facilitates maximum sulfate formation in JJA, more prevalent precipitation in JJA (Fig. 2) leads to enhanced wet removal of sulfate in eastern China. The result is a maximum of SO_4^{2-} in DJF and SON. Simulated concentrations of NO_3^- are generally higher than those of SO_4^{2-} in eastern China, which is likely caused by the overestimate of NH_3 emissions in that region (Wang et al., 2012b). The highest NO_3^- concentrations of 9–13 µg m^{-3} are simulated in DJF because of the relatively low temperatures and precipitation. In contrast, high temperatures and large rainfall in JJA lead to the lowest NO_3^- concentrations. Because of the excess amount of NH_3 in eastern China (Wang et al., 2012b), ammonium aerosol exists predominantly as ammonium sulfate or ammonium nitrate; its concentrations are simulated to be the highest (5–7 µg m^{-3}) in DJF. Predicted BC and OC concentrations are high in DJF and SON and low in MAM and JJA, again owing to the seasonal variation of precipitation (Fig. 2). Simulated $PM_{2.5}$ concentrations in DJF are about twice those in JJA in eastern China, with the highest values of 18–32 µg m^{-3} in DJF and of 9–18 µg m^{-3} in JJA. In the surface layer, NO_3^- is predicted to have been the most abundant aerosol species over eastern China in 1999–2001, followed by SO_4^{2-}, NH_4^+, OC, and BC.

3.3 Comparisons of simulated concentrations with measurements

Three previous studies have compared the simulated aerosol concentrations in GEOS-Chem with measurements taken during 2001–2009 in China (Zhang et al., 2010a; Wang et al., 2012b; Fu et al., 2012). At a horizontal resolution of 4° latitude by 5° longitude, Zhang et al. (2010a) found that GEOS-Chem tends to underestimate $PM_{2.5}$ aerosol concentrations in China, because measurements are usually taken in urban areas, whereas the simulated values represent grid cell averages. By using the one-way nested-grid capability of GEOS-Chem with a horizontal resolution of 0.5° latitude by 0.6674° longitude, Wang et al. (2012b) found that simulated concentrations of sulfate, nitrate, and ammonium at 22 sites in East Asia exhibited annual biases of −10 %, +31 %, and +35 %, respectively, and Fu et al. (2012) reported that the simulated annual mean concentrations of BC and OC averaged over rural and background sites were underestimated by 56 % and 76 %, respectively. Underestimation of BC in China was also found in all AEROCOM models (Koch et al., 2009), suggesting that emissions of carbonaceous aerosols are currently underestimated in China.

No publicly accessible in situ measurement network of aerosols in China exists (Chan and Yao, 2008). Therefore, we have compiled for model evaluation the monthly or seasonal mean measured concentrations of each aerosol species based on measurements reported in the literature. Most observations were conducted between 2001–2009 at urban sites (such as Beijing, Shanghai, and Guangzhou) and at a few rural sites (such as Fenghuangshan, Gaolanshan, and Lin'an). See Supplement for the locations of measurements. Scatter plots of simulated versus observed seasonal mean sulfate, nitrate, BC, and OC concentrations are displayed in Fig. 6. As anticipated, aerosol concentrations are generally underpredicted; the simulated concentrations of sulfate, nitrate, BC, and OC are about 35 %, 63 %, 29 %, and 18 % of the measured values, respectively. One notes the especially low levels of BC and OC simulated, as compared with measurements, indicating the inadequacy of current emission inventories for these species. Comparisons of simulated versus observed concentrations of all

aerosol species show relatively high correlation coefficients, with values of R^2 ranging from 0.77–0.87. These relatively high R^2 values indicate that the model captures the spatial distributions and seasonal variations of each aerosol species despite the general low bias in simulated concentrations. Again, one should bear in mind that predicted concentrations in this study have been averaged over 4° × 5° grid cells.

4 Predicted 2000–2050 changes in surface-layer aerosols in China

4.1 Effect of changes in climate alone

Figure 7 shows the predicted future changes in seasonal mean surface-layer O_3 and aerosol concentrations as a result of the future changes in climate alone. In DJF, O_3 concentrations are predicted to increase by 2–4 ppbv in southeastern China and decrease by 1–2 ppbv in northern China, which correspond well to the reduced clouds in southern China and the increases in clouds in northern plain (Fig. 3). The reductions in clouds lead to increases in solar radiation, which drive the photochemical production of O_3 (Langner et al., 2005; Jenong and Park, 2013). In MAM and SON, concentrations of O_3 exhibit reductions of 1–3 ppbv in eastern China, which again corresponds with the changes in clouds. In JJA, O_3 concentrations show increases of 1–3 ppbv in the whole eastern China because of a 33 % increase in biogenic emissions of NMVOC over 2000–2050. Sensitivity studies have shown that the increases in biogenic emissions can increase O_3 concentrations because most industrialized regions in China are VOC-limited (Han et al., 2005; Lin et al., 2008; Geng et al., 2011).

Simulated changes in concentrations of the aerosol species are within the range of -2.3 to $+1.7\,\mu g\,m^{-3}$ and exhibit similar spatial patterns in each of the four seasons. In DJF, concentrations of SO_4^{2-}, NH_4^+, BC, and OC are predicted to decrease by up to $1\,\mu g\,m^{-3}$ in central China and increase by $0.2–1\,\mu g\,m^{-3}$ in southeastern China, results that are consistent with the respective $+50\%$ and -40% predicted changes in precipitation in these two regions (Fig. 2). Predicted reductions in nitrate concentrations

of 1.5–2.3 μg m^{-3} in central China in DJF also result from the increase in temperature over 2000–2050 which leads to the shift of gas-aerosol equilibrium toward the gas phase. Concentrations of BC and OC are predicted to increase in southeastern China in MAM and throughout eastern China in JJA, despite increases in precipitation in those regions over 2000–2050 (Fig. 2), indicating that the future reductions in PBL height (Fig. 4) play a larger role than the changes in precipitation in influencing aerosol concentrations here. In SON, reductions in aerosol concentrations are predicted over eastern China, consistent with the projected increases in precipitation in that region.

As a result of the changes in individual aerosol species, PM$_{2.5}$ concentrations in DJF are predicted to exhibit increases of 1–2 μg m^{-3} in southeastern China but decreases of 3–5 μg m^{-3} in central China. Increases in PM$_{2.5}$ are predicted over a large fraction of eastern China in MAM and JJA, with maximum increases in the range of 2–4 μg m^{-3}. PM$_{2.5}$ shows general decreases of 1–3 μg m^{-3} in eastern China in SON. These estimated climate-induced changes in PM$_{2.5}$ concentrations over 2000–2050 represent about 10–20 % of the present-day values in those regions.

4.2 Effect of changes in anthropogenic emissions alone

The effect of projected changes in anthropogenic emissions over 2000–2050 alone is to generally increase O$_3$ concentrations in China in all seasons (Fig. 8). The predicted increases in O$_3$ in DJF are about 4 ppbv in eastern China and 4–12 ppbv in western China, which substantially exceed those due to climate change alone. The increases of O$_3$ of 4–12 ppbv occur over a large fraction of China in MAM and SON, with the largest increases of 12–23 ppbv simulated to occur in eastern China in JJA. These increases, except those over or near the Tibet Plateau, are consistent with the projected emission changes in China; anthropogenic emissions of NO$_x$ and NMVOCs are predicted to increase by 72 % and 86 % in eastern China (Table 1), respectively, in the scenario considered here. Over and in the vicinity of the Tibet Plateau, the large predicted increases

in O_3 are caused by transport from South Asia, which will be discussed further when we consider transboundary transport.

Year 2050 annual anthropogenic emissions of SO_2, BC, and OC are predicted to decrease by 29 %, 59 %, and 40 %, respectively, relative to the present-day values. Future concentrations of sulfate, BC, and OC in China are hence predicted to decrease (Fig. 8). The predicted reductions in sulfate aerosol lie within the range of 0.5–2 $\mu g\,m^{-3}$ throughout the year. Although the simulated present-day concentrations of BC and OC are lower than those of sulfate, the decreases in BC and OC are 0.5–2 $\mu g\,m^{-3}$ and 0.5–3.5 $\mu g\,m^{-3}$, respectively, in eastern China.

Unlike sulfate, BC, and OC, based on changes in emissions alone, nitrate concentrations are predicted to increase in the future due to changing anthropogenic emissions, with the largest increases of 1–2 $\mu g\,m^{-3}$ in DJF and 2–3.5 $\mu g\,m^{-3}$ in other seasons in eastern China. These increases can be explained by the 72 % assumed increase in annual anthropogenic NO_x emissions over 2000–2050 (Table 1) as well as the fact that the reduction in SO_2 favors the formation of ammonium nitrate. As a result, ammonium concentrations show increases of about 0.5 $\mu g\,m^{-3}$ over those locations with large increases in nitrate.

The net effect of the changes in all aerosol species owing to changes in emissions alone is an overall decrease in $PM_{2.5}$ concentrations in China except for the Tibet Plateau. Over eastern China, the projected largest decreases in $PM_{2.5}$ as a result of the future changes in emissions are 7–9.5 $\mu g\,m^{-3}$ in DJF, 1–4 $\mu g\,m^{-3}$ in MAM and JJA, and 2–7 $\mu g\,m^{-3}$ in SON, which are about 10–30 % reductions relative to the present-day values. As noted, the increase in $PM_{2.5}$ over or near the Tibet Plateau is caused by long-range transport from South Asia.

4.3 Effect of changes in both climate and anthropogenic emissions

Predicted future changes in O_3 and aerosols as a consequence of future changes in both climate and anthropogenic emissions are summarized in Fig. 9. For O_3, the effect

of projected future changes in anthropogenic emissions is dominant; large increases in O_3 of 15–25 ppbv are simulated in eastern China in JJA, with increases of 5–15 ppbv in a large fraction of China in other seasons. Climate change slightly mitigates the effect of changes in anthropogenic emissions on O_3 levels in MAM and SON, and enhances that of changes in anthropogenic emissions in JJA.

Concentrations of sulfate, BC, and OC in China are predicted to decrease in all seasons under future changes in both climate and anthropogenic emissions, although climate change can, to some extent, offset the effect of reductions in anthropogenic emissions on these species. In eastern China, concentrations of sulfate are predicted to decrease 1–3 $\mu g\,m^{-3}$ in DJF and SON and about 0.5–2 $\mu g\,m^{-3}$ in MAM and JJA, while those of BC and OC to decrease by 0.5–2 $\mu g\,m^{-3}$ and 0.5–3.5 $\mu g\,m^{-3}$, respectively, in all seasons.

For nitrate aerosols in eastern China, while climate change exerts an effect opposite to that of changes in anthropogenic emissions in DJF and SON, in MAM and JJA the effect of climate change enhances the changes due to emissions. As a result of changes in both climate and anthropogenic emissions, concentrations of nitrate are predicted to exhibit reductions of 0.5–1 $\mu g\,m^{-3}$ in central China in DJF and increases of 1–4 $\mu g\,m^{-3}$ in eastern China in other seasons.

The simulated 2000–2050 changes in $PM_{2.5}$ in DJF and SON are dominated by future changes in emissions; concentrations of $PM_{2.5}$ in eastern China are simulated to decrease by 2–9.5 $\mu g\,m^{-3}$. In MAM and JJA, climate change has a dominant role in influencing the future changes in aerosols in the lower reaches of Yangtze River, where increases of 1–5 $\mu g\,m^{-3}$ in $PM_{2.5}$ are simulated.

5 Simulated 2000–2050 changes in transboundary transport of aerosols

We next estimate 2000–2050 changes in aerosols fluxes into and out of China. These fluxes of aerosols are calculated through 3 vertical planes (Fig. 10): (1) the meridional plane along 135° E from 20 to 55° N that captures the outflow from eastern China to the

western Pacific, (2) the meridional plane along 75° E from 35 to 55° N that captures the inflow from Europe and Central Asia to China, and (3) the latitudinal plane along 20° N from 90 to 125° E to capture the transport to or from South Asia and Southeast Asia.

5.1 Outflow of aerosols from eastern China

5.1.1 Estimated present-day outflow

Simulated present-day seasonal and annual total fluxes of SO_4^{2-}, NO_3^-, NH_4^+, BC, OC, and $PM_{2.5}$ across the meridional plane along 135° E from 20 to 55° N are listed in Table 3. Among all aerosol species, the estimated present-day outflow of SO_4^{2-} of 5.1 Tg yr^{-1} across this plane is the largest, contributing 48 % of the annual outflow of $PM_{2.5}$. The estimated fluxes of NO_3^-, NH_4^+, BC, and OC account for 19 %, 15 %, 5 %, and 13 % of annual outflow of $PM_{2.5}$, respectively. Aerosol fluxes show strong seasonal variations. The outflow of SO_4^{2-} is simulated to peak in DJF, which results from the simulated high concentrations of sulfate (Fig. 5) and the strong westerlies (Fig. 11) in that season. All other aerosol species exhibit maximum outflow in MAM, a result that agrees with the conclusions from previous studies (Holzer et al., 2005). Heald et al. (2006) and Chin et al. (2007) reported that the export from Asia is most efficient in spring with nearly all East Asian air involved in transpacific transport. The outflow of aerosols is generally the weakest in JJA, as reported by Holzer et al. (2005) and Yu et al. (2008).

The pressure-latitude cross sections of the simulated fluxes of $PM_{2.5}$ at 135° E are shown in Fig. 11. The altitude range of the maximum fluxes of aerosols are found at 500–700 hPa in DJF and JJA and at 400–600 hPa in MAM and JJA. The locations of these maximum fluxes shift from 20–35° N in DJF and MAM to 30–50° N in JJA and SON, which are consistent with the changes in westerlies (Fig. 11). Our simulated vertical distributions of the strongest fluxes of aerosols agree with those reported by Wang et al. (2009), who showed that the transport to North America occurs mainly in the mid-to-upper troposphere.

5.1.2 Effect of changes in climate alone

Simulated future changes in seasonal and annual fluxes of SO_4^{2-}, NO_3^-, NH_4^+, BC, OC, and $PM_{2.5}$ through the meridional plane along $135°$ E are also listed in Table 3. As a result of the climate change alone, the annual fluxes of SO_4^{2-}, NO_3^-, NH_4^+, BC, OC, and $PM_{2.5}$ are simulated to change by -1.9%, -16.0%, -8.3%, -2.2%, -5.4% and -6.0%, respectively, relative to the present-day values. Nitrate aerosol outflow is projected to exhibit the largest reduction, because nitrate aerosol concentrations in China decrease significantly in a warmer climate (Fig. 7). The fluxes of all aerosol species show reductions in all seasons except MAM, when SO_4^{2-}, NH_4^+, BC, and $PM_{2.5}$ are simulated to increase by 11.9%, 0.5%, 1.4%, and 2.0%, respectively, as a result of the stronger westerlies throughout the troposphere in the latitude range of $28-50°$ N in the future atmosphere (Fig. 11).

5.1.3 Effect of changes in anthropogenic emissions alone

Annual fluxes of SO_4^{2-}, NO_3^-, NH_4^+, BC, OC, and $PM_{2.5}$ are simulated to change by -6.1%, $+26.4\%$, $+10.2\%$, -39.1%, -21.7% and -1.5%, respectively (Table 3), as a result of the changes in anthropogenic emissions alone. While nitrate and ammonium outflow fluxes exhibit large increases owing to the projected increases in concentrations in China (Fig. 8), the fluxes of SO_4^{2-}, BC, and OC decrease, corresponding to the decreases in concentrations of these species from the future projected decreases in emissions of SO_2, BC, and OC (Fig. 8). Consequently, the annual outflow of total $PM_{2.5}$ is estimated to exhibit a modest change of -1.5% over 2000–2050.

5.1.4 Effect of changes in both climate and anthropogenic emissions

Simulated year 2050 outflow fluxes of aerosols through the meridional plane along $135°$ E from 20 to $55°$ N with the future changes in both anthropogenic emissions and climate are listed in Table 3. The annual fluxes of SO_4^{2-}, NO_3^-, NH_4^+, BC, OC, and

PM$_{2.5}$ are simulated to change by −9.1 %, +4.2 %, +0.9 %, −41.3 %, −27.1 % and −9.0 %, respectively. Climate change slightly mitigates the effects of increases in NO$_x$ emissions on annual fluxes of NO$_3^-$ and NH$_4^+$, but enhances the effects of reductions in emissions of SO$_2$, BC, and OC on outflow of SO$_4^{2-}$, BC and OC.

As for future changes in seasonal mean fluxes of SO$_4^{2-}$, NO$_3^-$, NH$_4^+$, BC, and OC, the impact of future changes in emissions generally dominates over that of future changes in climate, except for sulfate in MAM, nitrate in MAM, and ammonium in DJF and JJA, when the impact of climate is larger (Table 3). With all aerosol species accounted for, the 2000–2050 changes in seasonal and annual outflow fluxes of PM$_{2.5}$ resulting from future climate alone always exceed those caused by future changes in emissions alone (Table 3), indicating that future climate change can be influential in estimates of future intercontinental transport of aerosols.

5.2 Inflow of aerosols to western China

5.2.1 Present-day inflow

Simulated present-day seasonal and annual fluxes of aerosols through the meridional plane along 75° E from 35° to 55° N are listed in Table 4. On an annual basis, the estimated fluxes of SO$_4^{2-}$, NO$_3^-$, NH$_4^+$, BC, and OC are 2.2, 0.5, 0.6, 0.1, and 0.3 Tg, respectively. The annual inflow of PM$_{2.5}$ is 3.8 Tg, which is about 35 % of the annual outflow of PM$_{2.5}$ from eastern China. The inflow of SO$_4^{2-}$ peaks in DJF, when simulated SO$_4^{2-}$ concentrations are high in Europe, and in MAM, when the westerlies are strong (Fig. 12). The fluxes of NH$_4^+$, BC, OC, and PM$_{2.5}$ all peak in MAM because of the dominant effect of strong westerlies in this season. The inflow of NO$_3^-$ is largest in JJA, when NO$_3^-$ concentrations are highest in Europe (not shown).

The pressure-latitude cross sections of the simulated fluxes of PM$_{2.5}$ at 75° E are shown in Fig. 12. The fluxes of aerosols are the largest north of 40° N, which is the

principal predicted transport path from Europe. The strongest inflow of all aerosol species is located at about 700 hPa in altitude.

5.2.2 Effect of changes in climate alone

Relative to the present-day values, the annual fluxes of SO_4^{2-}, NO_3^-, NH_4^+, BC, OC, and $PM_{2.5}$ through the meridional plane along 75° E from 35 to 55° N are simulated to change by +6.2 %, −25.4 %, −7.6 %, −0.8 %, −5.4 %, and −1.8 %, respectively, as a result of the climate change alone. As expected, the warmer future temperatures lead to large reductions of 18–33 % in estimated seasonal mean inflow of nitrate. The fluxes of SO_4^{2-}, BC, and $PM_{2.5}$ are simulated to increase by 15.4 %, 5.6 %, 8.6 % in DJF, as a result of the future stronger westerlies in DJF (Fig. 12). In MAM, the westerlies show small changes around 700 hPa, leading to little or no change in the fluxes of SO_4^{2-}, BC, OC, and $PM_{2.5}$. The westerlies are simulated to diminish significantly in the mid-higher troposphere north of 45° N in JJA and SON (Fig. 12), leading to reductions in inflow of all aerosol species in these two seasons.

5.2.3 Effect of changes in anthropogenic emissions alone

The annual fluxes of SO_4^{2-}, NO_3^-, NH_4^+, BC, OC, and $PM_{2.5}$ are simulated to change by +3 %, +93 %, +43 %, −23 %, −22 %, and +19 %, respectively (Table 4), as a result of the future changes in anthropogenic emissions alone. The magnitudes of changes in fluxes of NO_3^-, NH_4^+, BC, OC, and $PM_{2.5}$ by anthropogenic emissions alone are generally larger than those of changes by climate change alone on either a seasonal or annual mean basis. As a result of future changes in emissions, the seasonal fluxes of NO_3^- and NH_4^+ show large increases of 71–104 % and 21–59 %, respectively, those of BC and OC show large decreases of 18–29 % and 13–34 %, respectively, and the inflow of $PM_{2.5}$ is predicted to increase by about 20 % in all seasons (Table 4).

5.2.4 Effect of changes in both climate and anthropogenic emissions

Year 2050 inflow fluxes of aerosols through the meridional plane along 75° E calculated with the future changes in both anthropogenic emissions and climate are listed in Table 4. The annual fluxes of SO_4^{2-}, NO_3^-, NH_4^+, BC, and OC are simulated to change by +9 %, +53 %, +37 %, −24 %, and −27 %, respectively. Climate change mitigates the effects of increases in NO_x emissions on annual fluxes of NO_3^- and NH_4^+, but enhances the effects of changes in emissions of SO_2, BC, and OC. As a net result of the changes in inflow of all aerosol species, the annual inflow of $PM_{2.5}$ to western China is projected to increase by 15 % over 2000–2050 with future changes in both emissions and climate.

5.3 Transport of aerosols to/from southern China

5.3.1 Present-day transport

The simulated present-day seasonal and annual fluxes of aerosols through the latitudinal plane along 20° N from 90–125° E are listed in Table 5. The annual fluxes of SO_4^{2-}, NO_3^-, NH_4^+, BC, OC, and $PM_{2.5}$ are −0.13, −0.08, −0.03, +0.10, +0.69, and +0.55 Tg, respectively, with the positive (or negative) values indicating northward (or southward) transport of aerosols. The signs of the aerosol fluxes are determined by the directions of winds and the simulated distributions of aerosols. In DJF and SON, while southward fluxes of all aerosol species are found in the lower troposphere over 100–125° E because of the prevailing northerlies over eastern China, northward fluxes of aerosols are found through the depth of the troposphere over 90–100° E and in the upper troposphere over 100–125° E (Fig. 13). In MAM and JJA, the southerlies associated with the summer monsoon generally favor northward transport (Fig. 13). The fluxes of aerosols across the southern boundary of China are generally much smaller than those through the eastern and western boundaries; the annual inflow of $PM_{2.5}$ through the southern boundary is 0.55 Tg, which is 5 % of the annual outflow of $PM_{2.5}$ from eastern China and 15 % of the annual inflow to western China. One exception is that the fluxes of BC

and OC to China in MAM are amplified as a result of predominant biomass burning in South Asia in this season (Zhang et al., 2010b).

5.3.2 Effect of changes in climate alone

As a result of the future climate change alone, the annual southward fluxes of SO_4^{2-},
NO_3^-, NH_4^+ are simulated to increase by 69 %, 105 %, and 127 %, and the annual north-ward fluxes of BC, OC, and $PM_{2.5}$ are simulated to decrease by 16 %, 10 %, and 55 %, respectively, relative to the present-day values. In DJF, while the northerlies in the lower troposphere east of 100° E are predicted to be stronger, the southerlies west of 100° E become weaker (Fig. 13), both of which lead to larger future transport of SO_4^{2-}, NO_3^-,
NH_4^+, BC, and $PM_{2.5}$ from China to South Asia. In MAM, the northward fluxes of all aerosol species except for SO_4^{2-} are estimated to be smaller than those in present-day as a result of the weaker southerlies between 300–850 hPa over 90–110° E (Fig. 13). The flux of SO_4^{2-} in MAM increases by 7 % because the southward winds in the east of 115° E are projected to become weaker. In JJA, the southerlies associated with the
summer monsoon are simulated to strengthen in the future climate and hence favor the northward transport of aerosols. The fluxes of all aerosol species to South Asia in SON show reductions, which can be explained by the weaker northerlies in the future atmosphere (Fig. 13).

5.3.3 Effect of changes in anthropogenic emissions alone

The annual fluxes of SO_4^{2-} and NH_4^+ are simulated to change from a net southward outflow to a net northward inflow, as a result of the changes in anthropogenic emissions over 2000–2050 (Table 5). The annual southward flux of NO_3^- increases by 197 %, and the annual northward fluxes of BC, OC, and $PM_{2.5}$ increase by 42 %, 12 %, and 133 %, respectively. The annual fluxes of SO_4^{2-} and NH_4^+ exhibit large increases in northward
transport because of the large increases in aerosol concentrations in South Asia and Southeast Asia (Fig. 8), and the annual inflow of BC and OC also increases because

the reductions in carbonaceous aerosol concentrations in eastern China are projected to be larger than those in South Asia and Southeast Asia (Fig. 8). In contrast, the annual flux of NO_3^- exhibits southward outflow because of the large increases in NO_3^- levels in eastern China (Fig. 8).

5.3.4 Effect of changes in both climate and anthropogenic emissions

Simulated fluxes of aerosols through the latitudinal plane along $20°$ N from 90–125° E with the future changes in both anthropogenic emissions and climate are listed in Table 5. The year 2050 annual fluxes of SO_4^{2-}, NH_4^+, BC, OC, and $PM_{2.5}$ are simulated as northward into China, and the annual flux of NO_3^- is a southward out of China. The absolute values of annual fluxes of SO_4^{2-}, NO_3^-, NH_4^+, BC, OC, and $PM_{2.5}$ increase by 370 %, 359 %, 306 %, 30 %, 3 %, and 63 %, respectively, from present day to 2050. These changes in fluxes of all aerosol species are dominated by the contributions from changes in anthropogenic emissions. However, the role of future climate change can exceed that of future changes in emissions for the fluxes of NO_3^- in DJF and MAM, BC in DJF and JJA, as well as OC in DJF (Table 5).

6 Conclusions and discussions

We estimate changes in aerosol levels in China and the transboundary transport of aerosols in and out of China over the period 2000–2050 by using the global chemical transport model GEOS-Chem with meteorological input from the general circulation model GISS GCM 3 (at $4° \times 5°$ resolution) and changes in emissions based on the IPCC A1B scenario.

Simulated increases in temperature in China over 2000–2050 from the GISS GCM 3 range over 1–3 K. Projected changes in precipitation exhibit increases in northern China in DJF and over all of eastern China in JJA, which agree with those from the IPCC AR4 multi-model predictions for China under the A1B scenario (IPCC, 2007).

These projected changes in meteorological parameters alone are estimated to lead to changes in seasonal mean concentrations of individual aerosol species ranging from -2.3 to $+1.7\,\mu g\,m^{-3}$ over 2000–2050. The changes in sulfate, BC, and OC result mainly from the estimated changes in precipitation and PBL height. Future changes in nitrate and ammonium levels are also sensitive to the increase in temperature, especially in winter when the present-day concentrations of these two aerosol species are the highest among all four seasons. As a result of the projected changes in the levels of individual aerosol species, overall $PM_{2.5}$ concentrations are projected to exhibit wintertime (DJF) increases of $1-2\,\mu g\,m^{-3}$ in southeastern China, decreases of $3-5\,\mu g\,m^{-3}$ in central China, and spring and summer increases over a large portion of eastern China, with maximum increases in the range of $2-4\,\mu g\,m^{-3}$. $PM_{2.5}$ shows general decreases of $1-3\,\mu g\,m^{-3}$ in eastern China in the fall (SON). These estimated climate-induced changes in $PM_{2.5}$ concentrations over 2000–2050 represent about 10–20 % of the present-day values in those regions.

Relative to present day, year 2050 anthropogenic emissions of NO_x, SO_2, NH_3, OC, BC, CO, and NMVOCs in eastern China (20–55° N, 98–125° E) according to scenario A1B are estimated to change by $+72\%$, -29%, -12%, -40%, -59%, -7%, and $+86\%$, respectively. As a result of these changes in anthropogenic emissions alone, yearly decreases of $0.5-2\,\mu g\,m^{-3}$ in sulfate and of $0.5-2\,\mu g\,m^{-3}$ and $0.5-3.5\,\mu g\,m^{-3}$ in BC and OC, respectively, are estimated in eastern China. On the contrary, nitrate concentrations are predicted to increase, over 2000–2050 in eastern China, with the largest increases of $1-2\,\mu g\,m^{-3}$ in DJF and $2-3.5\,\mu g\,m^{-3}$ in other seasons. The projected net effect of the changes in all aerosol species to changes in emissions alone is an overall decrease in $PM_{2.5}$ concentrations in eastern China over 2000–2050. The largest seasonal decreases in $PM_{2.5}$ are $7-9.5\,\mu g\,m^{-3}$ in DJF, $1-4\,\mu g\,m^{-3}$ in MAM and JJA, and $2-7\,\mu g\,m^{-3}$ in SON, which represent about 10–30 % reductions relative to present-day values. Under the IPCC A1B scenario, future changes in anthropogenic emissions exert a larger effect on year 2050 $PM_{2.5}$ concentrations in eastern China than does projected future climate change.

Title Page

Abstract | Introduction

Conclusions | References

Tables | Figures

|◄ | ►|

◄ | ►

Back | Close

Full Screen / Esc

Printer-friendly Version

Interactive Discussion

Year 2050 estimated transboundary fluxes of aerosol species to and from China are sensitive to future changes in climate and emissions. The present-day flux of $PM_{2.5}$ from eastern China to the western Pacific (through the meridional plane along 135° E from 20 to 55° N) is simulated to be 10.6 Tg yr^{-1}, and the annual outflow of $PM_{2.5}$ is es-
5 timated to change by −6.0 %, −1.5 %, and −9.0 %, respectively, over 2000–2050 owing to future climate change alone, future changes in emissions alone, and future changes in both climate emissions. Climate change is predicted to have a larger impact on future fluxes of aerosols than changes in emissions. While annual fluxes of all aerosol species show reductions by climate change alone, future increases in outflow of nitrate
10 and ammonium offset to a large extent the future decreases in outflow of sulfate, BC, and OC, leading to a small negative change in annual outflow of $PM_{2.5}$ as a result of changes in emissions alone.

The present-day inflow of $PM_{2.5}$ aerosols from Europe and Central Asia to western China (the fluxes through the meridional plane along 75° E from 35 to 55° N) is calcu-
15 lated to be 3.8 Tg yr^{-1}. Over 2000–2050, the fluxes of nitrate and ammonium aerosols are estimated to increase largely as a result of future changes in emissions, leading to an overall 15 % estimated increase in annual inflow of $PM_{2.5}$ to western China as a result of future changes in both emissions and climate.

The present-day net transport of $PM_{2.5}$ aerosols across the southern boundary (the
20 latitudinal plane along 20° N from 90 to 125° E) is estimated as 0.6 Tg yr^{-1}, in which the fluxes of sulfate, nitrate, and ammonium are southward out of China and those of BC and OC are northward into China. Fluxes of BC and OC to China in MAM contribute to a large fraction of the annual inflow of $PM_{2.5}$, as a result of biomass burning in South Asia in this season. The annual flux of $PM_{2.5}$ across the southern boundary of
25 China is estimated to change by −55 %, +133 %, and +63 % over 2000–2050 owing to climate change alone, changes in emissions alone, and changes in both climate and emissions, respectively.

Full Screen / Esc

Printer-friendly Version

Interactive Discussion

Results from the present study indicate that it is important to consider climate change in long-term air quality planning, for both domestic air quality in China and long-range transport of aerosols.

Supplementary material related to this article is available online at: http://www.atmos-chem-phys-discuss.net/13/6501/2013/ acpd-13-6501-2013-supplement.pdf.

References

Alexander, B., Park, R. J., Jacob, D. J., Li, Q. B., Yantosca, R. M., Savarino, J., Lee, C. C. W., and Thiemens, M. H.: Sulfate formation in sea-salt aerosols: constraints from oxygen isotopes, J. Geophys. Res.-Atmos., 110, D10307, doi:10.1029/2004jd005659, 2005.

Andersson, C. and Engardt, M.: European ozone in a future climate: importance of changes in dry deposition and isoprene emissions, J. Geophys. Res.-Atmos., 115, D02303, doi:10.1029/2008jd011690, 2010.

Bauer, S. E., Koch, D., Unger, N., Metzger, S. M., Shindell, D. T., and Streets, D. G.: Nitrate aerosols today and in 2030: a global simulation including aerosols and tropospheric ozone, Atmos. Chem. Phys., 7, 5043–5059, doi:10.5194/acp-7-5043-2007, 2007.

Bey, I., Jacob, D. J., Yantosca, R. M., Logan, J. A., Field, B. D., Fiore, A. M., Li, Q. B., Liu, H. G. Y., Mickley, L. J., and Schultz, M. G.: Global modeling of tropospheric chemistry with assimilated meteorology: model description and evaluation, J. Geophys. Res.-Atmos., 106, 23073–23095, 2001.

Cao, J. J., Shen, Z.-X., Chow, J. C., Watson, J. G., Lee, S.-C., Tie, X.-X., Ho, K.-F., Wang, G.-H., and Han, Y.-M.: Winter and summer $PM_{2.5}$ chemical compositions in fourteen Chinese cities, J. Air Waste Manage. Assoc., 62, 1214–1226, 2012.

Chan, C. K. and Yao, X.: Air pollution in mega cities in China, Atmos. Environ., 42, 1–42, doi:10.1016/j.atmosenv.2007.09.003, 2008.

Chang, H. H., Zhou, J. W., and Fuentes, M.: Impact of climate change on ambient ozone level and mortality in southeastern United States, Int. J. Env. Res. Pub. He., 7, 2866–2880, doi:10.3390/ijerph7072866, 2010.

Chin, Mian, Diehl, T., Ginoux, P., and Malm, W.: Intercontinental transport of pollution and dust aerosols: implications for regional air quality, Atmos. Chem. Phys., 7, 5501–5517, doi:10.5194/acp-7-5501-2007, 2007.

Clarke, A. D., Collins, W. G., Rasch, P. J., Kapustin, V. N., Moore, K., Howell, S., and Fuelberg, H. E.: Dust and pollution transport on global scales: aerosol measurements and model predictions, J. Geophys. Res.-Atmos., 106, 32555–32569, doi:10.1029/2000jd900842, 2001.

Day, M. C. and Pandis, S. N.: Predicted changes in summertime organic aerosol concentrations due to increased temperatures, Atmos. Environ., 45, 6546–6556, doi:10.1016/j.atmosenv.2011.08.028, 2011.

Duncan Fairlie, T., Jacob, D. J., and Park, R. J.: The impact of transpacific transport of mineral dust in the United States, Atmos. Environ., 41, 1251–1266, doi:10.1016/j.atmosenv.2006.09.048, 2007.

Fu, T. M., Cao, J. J., Zhang, X. Y., Lee, S. C., Zhang, Q., Han, Y. M., Qu, W. J., Han, Z., Zhang, R., Wang, Y. X., Chen, D., and Henze, D. K.: Carbonaceous aerosols in China: top-down constraints on primary sources and estimation of secondary contribution, Atmos. Chem. Phys., 12, 2725–2746, doi:10.5194/acp-12-2725-2012, 2012.

Geng, F., Tie, X., Guenther, A., Li, G., Cao, J., and Harley, P.: Effect of isoprene emissions from major forests on ozone formation in the city of Shanghai, China, Atmos. Chem. Phys., 11, 10449–10459, doi:10.5194/acp-11-10449-2011, 2011.

Guenther, A., Hewitt, C. N., Erickson, D., Fall, R., Geron, C., Graedel, T., Harley, P., Klinger, L., Lerdau, M., Mckay, W. A., Pierce, T., Scholes, B., Steinbrecher, R., Tallamraju, R., Taylor, J., and Zimmerman, P.: A global-model of natural volatile organic-compound emissions, J. Geophys. Res.-Atmos., 100, 8873–8892, 1995.

Title Page

Abstract | Introduction

Conclusions | References

Tables | Figures

|◄ | ►|

◄ | ►

Back | Close

Full Screen / Esc

Printer-friendly Version

Interactive Discussion

Han, Z. W., Ueda, H., and Matsuda, K.: Model study of the impact of biogenic emission on regional ozone and the effectiveness of emission reduction scenarios over eastern China, Tellus B, 57, 12–27, doi:10.1111/j.1600-0889.2005.00132.x, 2005.

Heald, C. L., Jacob, D. J., Park, R. J., Alexander, B., Fairlie, T. D., Yantosca, R. M., and Chu, D. A.: Transpacific transport of Asian anthropogenic aerosols and its impact on surface air quality in the United States, J. Geophys. Res.-Atmos., 111, D14310, doi:10.1029/2005jd006847, 2006.

Henze, D. K. and Seinfeld, J. H.: Global secondary organic aerosol from isoprene oxidation, Geophys. Res. Lett., 33, L09812, doi:10.1029/2006gl025976, 2006.

Henze, D. K., Seinfeld, J. H., Ng, N. L., Kroll, J. H., Fu, T.-M., Jacob, D. J., and Heald, C. L.: Global modeling of secondary organic aerosol formation from aromatic hydrocarbons: high- vs. low-yield pathways, Atmos. Chem. Phys., 8, 2405–2420, doi:10.5194/acp-8-2405-2008, 2008.

Hogrefe, C., Lynn, B., Civerolo, K., Ku, J. Y., Rosenthal, J., Rosenzweig, C., Goldberg, R., Gaffin, S., Knowlton, K., and Kinney, P. L.: Simulating changes in regional air pollution over the eastern United States due to changes in global and regional climate and emissions, J. Geophys. Res.-Atmos., 109, D22301, doi:10.1029/2004jd004690, 2004.

Holzer, M., Hall, T. M., and Stull, R. B.: Seasonality and weather-driven variability of transpacific transport, J. Geophys. Res.-Atmos., 110, D23103, doi:10.1029/2005jd006261, 2005.

Huebert, B. J., Phillips, C. A., Zhuang, L., Kjellstrom, E., Rodhe, H., Feichter, J., and Land, C.: Long-term measurements of free-tropospheric sulfate at Mauna Loa: comparison with global model simulations, J. Geophys. Res.-Atmos., 106, 5479–5492, doi:10.1029/2000jd900627, 2001.

Jacob, D. J. and Winner, D. A.: Effect of climate change on air quality, Atmos. Environ., 43, 51–63, doi:10.1016/j.atmosenv.2008.09.051, 2009.

Jeong, J. I. and Park, R. J.: Effects of the meteorological variability on regional air quality in East Asia, Atmos. Environ., 69, 46–55, 2013.

Jordan, C. E., Dibb, J. E., Anderson, B. E., and Fuelberg, H. E.: Uptake of nitrate and sulfate on dust aerosols during TRACE-P, J. Geophys. Res.-Atmos., 108, 1–10, 8817, doi:10.1029/2002jd003101, 2003.

Juda-Rezler, K., Reizer, M., Huszar, P., Krüger, B. C., Zanis, P., Syrakov, D., Katragkou, E., Trapp, W., Melas, D., Chervenkov, H., Tegoulias, I., and Halenka, T.: Modelling the effects

of climate change on air quality over Central and Eastern Europe: concept, evaluation and projections, Clim. Res., 53, 179–203, doi:10.3354/cr01072, 2012.

Katragkou, E., Zanis, P., Kioutsioukis, I., Tegoulias, I., Melas, D., Krüger, B. C., and Coppola, E.: Future climate change impacts on summer surface ozone from regional climate-air quality simulations over Europe, J. Geophys. Res.-Atmos., 116, D22307, doi:10.1029/2011jd015899, 2011.

Koch, D., Schulz, M., Kinne, S., McNaughton, C., Spackman, J. R., Balkanski, Y., Bauer, S., Berntsen, T., Bond, T. C., Boucher, O., Chin, M., Clarke, A., De Luca, N., Dentener, F., Diehl, T., Dubovik, O., Easter, R., Fahey, D. W., Feichter, J., Fillmore, D., Freitag, S., Ghan, S., Ginoux, P., Gong, S., Horowitz, L., Iversen, T., Kirkevåg, A., Klimont, Z., Kondo, Y., Krol, M., Liu, X., Miller, R., Montanaro, V., Moteki, N., Myhre, G., Penner, J. E., Perlwitz, J., Pitari, G., Reddy, S., Sahu, L., Sakamoto, H., Schuster, G., Schwarz, J. P., Seland, Ø., Stier, P., Takegawa, N., Takemura, T., Textor, C., van Aardenne, J. A., and Zhao, Y.: Evaluation of black carbon estimations in global aerosol models, Atmos. Chem. Phys., 9, 9001–9026, doi:10.5194/acp-9-9001-2009, 2009.

Lam, Y. F., Fu, J. S., Wu, S., and Mickley, L. J.: Impacts of future climate change and effects of biogenic emissions on surface ozone and particulate matter concentrations in the United States, Atmos. Chem. Phys., 11, 4789–4806, doi:10.5194/acp-11-4789-2011, 2011.

Langner, J., Bergström, R., and Foltescu, V.: Impact of climate change on surface ozone and deposition of sulphur and nitrogen in Europe, Atmos. Environ., 39, 1129–1141, 2005.

Langner, J., Engardt, M., Baklanov, A., Christensen, J. H., Gauss, M., Geels, C., Hedegaard, G. B., Nuterman, R., Simpson, D., Soares, J., Sofiev, M., Wind, P., and Zakey, A.: A multi-model study of impacts of climate change on surface ozone in Europe, Atmos. Chem. Phys., 12, 10423–10440, doi:10.5194/acp-12-10423-2012, 2012.

Li, J., Wang, Z. F., Akimoto, H., Gao, C., Pochanart, P., and Wang, X. Q.: Modeling study of ozone seasonal cycle in lower troposphere over east Asia, J. Geophys. Res.-Atmos., 112, D22S25, doi:10.1029/2006JD008209, 2007.

Liao, H., Chen, W.-T., and Seinfeld, J. H.: Role of climate change in global predictions of future tropospheric ozone and aerosols, J. Geophys. Res., 111, D12304, doi:10.1029/2005jd006852, 2006.

Liao, H., Henze, D. K., Seinfeld, J. H., Wu, S. L., and Mickley, L. J.: Biogenic secondary organic aerosol over the United States: comparison of climatological simulations with observations, J. Geophys. Res.-Atmos., 112, D06201, doi:10.1029/2006jd007813, 2007.

Title Page

Abstract | Introduction

Conclusions | References

Tables | Figures

|◀ | ▶|

◀ | ▶

Back | Close

Full Screen / Esc

Printer-friendly Version

Interactive Discussion

Lin, J. T., Patten, K. O., Hayhoe, K., Liang, X. Z., and Wuebbles, D. J.: Effects of future climate and biogenic emissions changes on surface ozone over the United States and China, J. Appl. Meteorol. Clim., 47, 1888–1909, doi:10.1175/2007jamc1681.1, 2008.

Matsui, H., Koike, M., Kondo, Y., Takegawa, N., Kita, K., Miyazaki, Y., Hu, M., Chang, S. Y., Blake, D. R., Fast, J. D., Zaveri, R. A., Streets, D. G., Zhang, Q., and Zhu, T.: Spatial and temporal variations of aerosols around Beijing in summer 2006: model evaluation and source apportionment, J. Geophys. Res.-Atmos., 114, D00g13, doi:10.1029/2008jd010906, 2009.

Maxwell-Meier, K., Weber, R., Song, C., Orsini, D., Ma, Y., Carmichael, G. R., and Streets, D. G.: Inorganic composition of fine particles in mixed mineral dust-pollution plumes observed from airborne measurements during ACE-Asia, J. Geophys. Res.-Atmos., 109, D19s07, doi:10.1029/2003jd004464, 2004.

Murazaki, K., and Hess, P.: How does climate change contribute to surface ozone change over the United States?, J. Geophys. Res.-Atmos., 111, D05301, doi:10.1029/2005jd005873, 2006.

Nakicenovic, N. and Swart, R. (Eds.): Special Report on Emissions Scenarios, 570 pp., Cambridge Univ. Press, New York, 2000.

Park, R. J.: Natural and transboundary pollution influences on sulfate-nitrate-ammonium aerosols in the United States: implications for policy, J. Geophys. Res., 109, D15204, doi:10.1029/2003jd004473, 2004.

Park, R. J., Jacob, D. J., Chin, M., and Martin, R. V.: Sources of carbonaceous aerosols over the United States and implications for natural visibility, J. Geophys. Res.-Atmos., 108, 4355, doi:10.1029/2002jd003190, 2003.

Price, C. and Rind, D.: A simple lightning parameterization for calculating global lightning distributions, J. Geophys. Res.-Atmos., 97, 9919–9933, 1992.

Price, H. U., Jaffe, D. A., Doskey, P. V., McKendry, I., and Anderson, T. L.: Vertical profiles of O_3, aerosols, CO and NMHCs in the Northeast Pacific during the TRACE-P and ACE-ASIA experiments, J. Geophys. Res.-Atmos., 108, 8799, doi:10.1029/2002jd002930, 2003.

Prospero, J. M., Savoie, D. L., and Arimoto, R.: Long-term record of nss-sulfate and nitrate in aerosols on Midway Island, 1981–2000: evidence of increased (now decreasing?) anthropogenic emissions from Asia, J. Geophys. Res.-Atmos., 108, 4019, doi:10.1029/2001jd001524, 2003.

Title Page

Abstract | Introduction

Conclusions | References

Tables | Figures

◄ | ►

◄ | ►

Back | Close

Full Screen / Esc

Printer-friendly Version

Interactive Discussion

Pye, H. O. T., Liao, H., Wu, S., Mickley, L. J., Jacob, D. J., Henze, D. K., and Seinfeld, J. H.: Effect of changes in climate and emissions on future sulfate-nitrate-ammonium aerosol levels in the United States, J. Geophys. Res.-Atmos., 114, D01205, doi:10.1029/2008jd010701, 2009.

Qu, W. J., Arimoto, R., Zhang, X. Y., Zhao, C. H., Wang, Y. Q., Sheng, L. F., and Fu, G.: Spatial distribution and interannual variation of surface PM_{10} concentrations over eighty-six Chinese cities, Atmos. Chem. Phys., 10, 5641–5662, doi:10.5194/acp-10-5641-2010, 2010.

Racherla, P. N. and Adams, P. J.: The response of surface ozone to climate change over the Eastern United States, Atmos. Chem. Phys., 8, 871–885, doi:10.5194/acp-8-871-2008, 2008.

Reuten, C., Ainslie, B., Steyn, D. G., Jackson, P. L., and McKendry, I.: Impact of climate change on ozone pollution in the lower Fraser Valley, Canada, Atmos. Ocean., 50, 42–53, doi:10.1080/07055900.2011.643444, 2012.

Rind, D., Lerner, J., Jonas, J., and McLinden, C.: Effects of resolution and model physics on tracer transports in the NASA Goddard Institute for Space Studies general circulation models, J. Geophys. Res.-Atmos., 112, D09315, doi:10.1029/2006jd007476, 2007.

Rosenstiel, T. N., Potosnak, M. J., Griffin, K. L., Fall, R., and Monson, R. K.: Increased CO_2 uncouples growth from isoprene emission in an agriforest ecosystem, Nature, 421, 256–259, doi:10.1038/Nature01312, 2003.

Steiner, A. L., Tonse, S., Cohen, R. C., Goldstein, A. H., and Harley, R. A.: Influence of future climate and emissions on regional air quality in California, J. Geophys. Res.-Atmos., 111, D18303, doi:10.1029/2005jd006935, 2006.

Streets, D. G., Bond, T. C., Carmichael, G. R., Fernandes, S. D., Fu, Q., He, D., Klimont, Z., Nelson, S. M., Tsai, N. Y., Wang, M. Q., Woo, J. H., and Yarber, K. F.: An inventory of gaseous and primary aerosol emissions in Asia in the year 2000, J. Geophys. Res.-Atmos., 108, 8809, doi:10.1029/2002jd003093, 2003.

Streets, D. G., Bond, T. C., Lee, T., and Jang, C.: On the future of carbonaceous aerosol emissions, J. Geophys. Res.-Atmos., 109, D24212, doi:10.1029/2004jd004902, 2004.

Tai, A. P. K., Mickley, L. J., and Jacob, D. J.: Impact of 2000–2050 climate change on fine particulate matter ($PM_{2.5}$) air quality inferred from a multi-model analysis of meteorological modes, Atmos. Chem. Phys., 12, 11329–11337, doi:10.5194/acp-12-11329-2012, 2012a.

Tai, A. P. K., Mickley, L. J., Jacob, D. J., Leibensperger, E. M., Zhang, L., Fisher, J. A., and Pye, H. O. T.: Meteorological modes of variability for fine particulate matter ($PM_{2.5}$) air quality

in the United States: implications for PM$_{2.5}$ sensitivity to climate change, Atmos. Chem. Phys., 12, 3131–3145, doi:10.5194/acp-12-3131-2012, 2012b.

Tie, X. X. and Cao, J. J.: Erratum to "Aerosol pollution in China: Present and future impact on environment", Particuology, 8, 79–79, doi:10.1016/j.partic.2009.12.001, 2010.

Unger, N., Shindell, D. T., Koch, D. M., Amann, M., Cofala, J., and Streets, D. G.: Influences of man-made emissions and climate changes on tropospheric ozone, methane, and sulfate at 2030 from a broad range of possible futures, J. Geophys. Res.-Atmos., 111, D12313, doi:10.1029/2005jd006518, 2006.

Wang, K., Zhang, Y., Jang, C., Phillips, S., and Wang, B.: Modeling intercontinental air pollution transport over the trans-Pacific region in 2001 using the Community Multiscale Air Quality modeling system, J. Geophys. Res.-Atmos., 114, D04307, doi:10.1029/2008jd010807, 2009.

Wang, T., Cheung, V. T. F., Anson, M., and Li, Y. S.: Ozone and related gaseous pollutants in the boundary layer of eastern China: overview of the recent measurements at a rural site, Geophys. Res. Lett., 28, 2373–2376, 2001.

Wang, Y., McElroy, M. B., Munger, J. W., Hao, J., Ma, H., Nielsen, C. P., and Chen, Y.: Variations of O$_3$ and CO in summertime at a rural site near Beijing, Atmos. Chem. Phys., 8, 6355–6363, doi:10.5194/acp-8-6355-2008, 2008.

Wang, Y., Zhang, Q. Q., He, K., Zhang, Q., and Chai, L.: Sulfate-nitrate-ammonium aerosols over China: response to 2000–2015 emission changes of sulfur dioxide, nitrogen oxides, and ammonia, Atmos. Chem. Phys. Discuss., 12, 24243–24285, doi:10.5194/acpd-12-24243-2012, 2012.

Wang, Y., Shen, L., Wu, S., Mickley, L. J., He, J., and Hao, J.: Sensitivity of surface ozone over China to 2000–2050 global changes of climate and emissions, Atmos. Environ., in review, 2013.

Wang, Y. H., Jacob, D. J., and Logan, J. A.: Global simulation of tropospheric O$_3$-NO$_x$-hydrocarbon chemistry. 1. Model formulation, J. Geophys. Res.-Atmos., 103, 10713–10725, 1998.

Wild, O. and Akimoto, H.: Intercontinental transport of ozone and its precursors in a three-dimensional global CTM, J. Geophys. Res.-Atmos., 106, 27729–27744, doi:10.1029/2000jd000123, 2001.

Wu, S. L., Mickley, L. J., Jacob, D. J., Logan, J. A., Yantosca, R. M., and Rind, D.: Why are there large differences between models in global budgets of tropospheric ozone?, J. Geophys. Res.-Atmos., 112, D05302, doi:10.1029/2006jd007801, 2007.

Wu, S. L., Mickley, L. J., Leibensperger, E. M., Jacob, D. J., Rind, D., and Streets, D. G.: Effects of 2000–2050 global change on ozone air quality in the United States, J. Geophys. Res.-Atmos., 113, D06302, doi:10.1029/2007jd008917, 2008.

Yienger, J. J. and Levy, H.: Empirical-model of global soil-biogenic NO_x emissions, J. Geophys. Res.-Atmos., 100, 11447–11464, 1995.

Yu, H. B., Remer, L. A., Chin, M., Bian, H. S., Kleidman, R. G., and Diehl, T.: A satellite-based assessment of transpacific transport of pollution aerosol, J. Geophys. Res.-Atmos., 113, D14s12, doi:10.1029/2007jd009349, 2008.

Zhang, L., Liao, H., and Li, J. P.: Impacts of Asian summer monsoon on seasonal and inter-annual variations of aerosols over eastern China, J. Geophys. Res.-Atmos., 115, D00k05, doi:10.1029/2009jd012299, 2010a.

Zhang, L., Liao, H., and Li, J.: Impact of the Southeast Asian summer monsoon strength on the outflow of aerosols from South Asia, Ann. Geophys., 28, 277–287, doi:10.5194/angeo-28-277-2010, 2010b.

Zhu, J. L., Liao, H., and Li, J. P.: Increases in aerosol concentrations over eastern China due to the decadal-scale weakening of the East Asian summer monsoon, Geophys. Res. Lett., 39, L09809, doi:10.1029/2012gl051428, 2012.

Table 1. Present-day and year 2050 (IPCC A1B Scenario) predicted emissions of aerosol precursors and aerosols. The domain of eastern China is (20–55° N, 98–125° E).

Species	Global			Eastern China		
	2000	2050	Change, %	2000	2050	Change, %
NO_x $(Tg\,N\,yr^{-1})$						
Aircraft	0.5	0.5	0.0	0.02	0.02	0.0
Fossil fuel	23.7	47.9	+102.0	3.15	6.21	+97.1
Biomass burning	6.5	8.1	+24.6	0.30	0.34	+13.3
Biofuel	2.2	2.1	−4.5	0.53	0.36	−32.1
Fertilizer	0.5	0.9	+80.0	0.06	0.04	−33.3
Total	33.4	59.5	+78.1	4.06	6.97	+71.7
CO $(Tg\,CO\,yr^{-1})$						
Fossil fuel	420.1	413.6	−1.5	104.26	94.04	−9.8
Biomass burning	458.8	749.6	+63.4	21.69	34.46	+58.9
Biofuel	175.6	168.9	−3.8	46.34	31.24	−32.6
Total	1054.5	1332.1	+26.3	172.29	159.74	−7.3
NMVOCs $(Tg\,C\,yr^{-1})$						
Anthropogenic	24.5	42.2	+72.2	2.45	6.52	+166
Biomass burning	3.1	5.1	+64.5	0.14	0.23	+64.3
Biofuel	7.2	6.9	−4.2	1.65	1.12	−32.1
Total	34.8	54.2	+55.7	4.24	7.87	+85.6
SO_2 $(Tg\,S\,yr^{-1})$						
Aircraft	0.1	0.1	0.0	< 0.01	< 0.01	0.0
Anthropogenic	66.1	88.7	+34.2	13.83	9.81	−29.1
Biomass burning	1.2	2.0	+66.7	0.06	0.09	+50.0
Biofuel	0.3	0.3	0.0	0.07	0.05	−28.6
Ship	4.2	5.4	+28.6	0.03	0.05	+66.7
Total	71.9	96.5	+34.2	13.99	10.00	−28.5
NH_3 $(Tg\,N\,yr^{-1})$						
Agricultural	33.3	50.4	+51.4	6.68	5.9	−11.7
Biomass burning	5.9	6.1	+3.4	0.26	0.28	+7.7
Biofuel	1.6	1.7	+6.3	0.32	0.22	−31.3
Total	40.8	58.2	+42.6	7.26	6.4	−11.8
OC $(Tg\,C\,yr^{-1})$						
Fossil fuel	2.5	0.9	−64.0	0.58	0.16	−72.4
Biomass burning	21.6	21.8	+0.9	1.10	1.08	−1.8
Biofuel	6.4	2.7	−57.8	1.31	0.56	−57.3
Total	30.5	25.4	−16.7	2.99	1.80	−39.8
BC $(Tg\,C\,yr^{-1})$						
Fossil fuel	3.1	2.0	−35.5	0.84	0.27	−67.9
Biomass burning	2.6	2.7	+3.8	0.13	0.13	0.0
Biofuel	1.5	0.6	−60.0	0.36	0.15	−58.3
Total	7.2	5.3	−26.4	1.33	0.55	−58.6

Table 2. Simulated changes in natural emissions due to predicted climate change (IPCC A1B Scenario). The domain of eastern China is (20–55° N, 98–125° E).

Species	Global			Eastern China		
	2000	2050	Change, %	2000	2050	Change, %
NO_x (Tg N yr^{-1})						
Lightning	4.8	5.6	+16.7	0.30	0.38	+26.7
Soil	6.3	7.3	+15.9	0.31	0.35	+12.9
Total	11.1	12.9	+16.2	0.61	0.73	+19.7
Biogenic HCs (Tg C yr^{-1})						
Isoprene	440.3	563.6	+28.0	22.47	27.30	+21.5
Monoterpenes	127.9	156.9	+22.7	7.00	8.20	+11.4
Acetone	44.8	53.4	+19.2	1.45	1.72	+18.6
Propene	12.6	16.1	+27.8	0.64	0.78	+21.9
Methyl Butenol	6.6	8.3	+25.8	1.42	1.75	+23.2
Total	632.2	798.3	+26.3	32.98	39.75	+20.5

Title Page

Abstract | Introduction

Conclusions | References

Tables | Figures

|◀ | ▶|

◀ | ▶

Back | Close

Full Screen / Esc

Printer-friendly Version

Interactive Discussion

Table 3. Simulated outflow of aerosols from eastern China through the meridional plane along 135° E from 20 to 55° N. Numbers in the parentheses are percentage changes relative to the present-day fluxes.

Species		2000[a] (Tg)	Outflow from Eastern China 2050[b] (Tg)	2050[c] (Tg)	2050[d] (Tg)
SO_4^{2-}	DJF	2.155	1.964(−8.8 %)	2.094(−2.8 %)	1.928(−10.4 %)
	MAM	1.437	1.608(+11.9 %)	1.469(−2.3 %)	1.558(+8.4 %)
	JJA	0.425	0.399(−6.3 %)	0.340(−20.4 %)	0.321(−24.6 %)
	SON	1.088	1.036(−5.0 %)	0.893(−17.9 %)	0.835(−23.4 %)
	Annual	5.105	5.007(−1.9 %)	4.797(−6.1 %)	4.641(−9.1 %)
NO_3^-	DJF	0.513	0.426(−17 %)	0.616(+19.9 %)	0.484(−5.8 %)
	MAM	0.775	0.692(−10.5 %)	0.836(+8.1 %)	0.768(−0.8 %)
	JJA	0.399	0.312(−21.8 %)	0.546(+36.8 %)	0.430(+7.5 %)
	SON	0.305	0.240(−21.0 %)	0.487(+60.4 %)	0.39(+28.7 %)
	Annual	1.992	1.671(−16.0 %)	2.514(+26.4 %)	2.073(+4.2 %)
NH_4^+	DJF	0.439	0.340(−8.9 %)	0.474(+8.2 %)	0.433(−1.4 %)
	MAM	0.591	0.593(+0.5 %)	0.655(+10.7 %)	0.657(+11.2 %)
	JJA	0.275	0.232(−16.3 %)	0.284(+3.3 %)	0.237(−14.1 %)
	SON	0.284	0.234(−17.9 %)	0.339(+18.9 %)	0.278(−2.1 %)
	Annual	1.589	1.458(−8.3 %)	1.752(+10.2 %)	1.605(+0.9 %)
BC	DJF	0.174	0.164(−5.2 %)	0.096(−44.8 %)	0.090(−48.3 %)
	MAM	0.212	0.215(+1.4 %)	0.152(−28.2 %)	0.150(−29.6 %)
	JJA	0.065	0.064(−4.5 %)	0.033(−50.0 %)	0.032(−50.0 %)
	SON	0.085	0.082(−3.6 %)	0.044(−46.4 %)	0.041(−50.0 %)
	Annual	0.536	0.525(−2.2 %)	0.327(−39.1 %)	0.315(−41.3 %)
OC	DJF	0.374	0.342(−9.6 %)	0.244(−35.2 %)	0.217(−42.4 %)
	MAM	0.643	0.621(−3.3 %)	0.593(−7.5 %)	0.562(−12.6 %)
	JJA	0.163	0.162(0.0 %)	0.117(−27.8 %)	0.116(−27.8 %)
	SON	0.161	0.148(−9.3 %)	0.095(−40.7 %)	0.084(−48.1 %)
	Annual	1.341	1.269(−5.4 %)	1.050(−21.7 %)	0.978(−27.1 %)
$PM_{2.5}$	DJF	3.656	3.295(−9.9 %)	3.523(−3.7 %)	3.151(−13.9 %)
	MAM	3.657	3.728(+2.0 %)	3.705(+1.3 %)	3.695(+1.1 %)
	JJA	1.328	1.169(−12.0 %)	1.320(−0.7 %)	1.137(−14.4 %)
	SON	1.924	1.739(−9.5 %)	1.857(−3.4 %)	1.629(−15.3 %)
	Annual	10.565	9.933(−6.0 %)	10.404(−1.5 %)	9.612(−9.0 %)

[a] Seasonal and annual total fluxes averaged over 1999–2001.
[b] Year 2050 fluxes simulated with climate change alone.
[c] Year 2050 fluxes simulated with changes in anthropogenic emissions alone.
[d] Year 2050 fluxes simulated with changes in both climate and anthropogenic emissions.

Table 4. Simulated inflow of aerosols to western China through the meridional plane along 75° E from 35 to 55° N. Numbers in the parentheses are percentage changes relative to the present-day fluxes.

Species		2000[a] (Tg)	Inflow to Western China 2050[b] (Tg)	2050[c] (Tg)	2050[d] (Tg)
SO_4^{2-}	DJF	0.712	0.822(+15.4 %)	0.821(+15.3 %)	0.845(+18.7 %)
	MAM	0.703	0.749(+6.5 %)	0.719(+2.3 %)	0.781(+11.1 %)
	JJA	0.273	0.253(−7.3 %)	0.225(−17.6 %)	0.238(−12.8 %)
	SON	0.520	0.520(0.0 %)	0.519(−0.2 %)	0.538(+3.4 %)
	Annual	2.208	2.344(+6.2 %)	2.284(+3.4 %)	2.402(+8.8 %)
NO_3^-	DJF	0.073	0.049(−32.9 %)	0.134(+83.6 %)	0.099(+35.6 %)
	MAM	0.138	0.101(−26.8 %)	0.282(+104.3 %)	0.215(+55.8 %)
	JJA	0.227	0.169(−25.6 %)	0.388(+70.9 %)	0.310(+36.6 %)
	SON	0.101	0.083(−17.8 %)	0.238(+135.6 %)	0.200(+98.0 %)
	Annual	0.539	0.402(−25.4 %)	1.042(+93.3 %)	0.824(+52.9 %)
NH_4^+	DJF	0.107	0.106(−0.9 %)	0.170(+58.9 %)	0.168(+57.0 %)
	MAM	0.171	0.165(−3.5 %)	0.247(+44.4 %)	0.244(+42.7 %)
	JJA	0.157	0.133(−15.3 %)	0.190(+21.0 %)	0.172(+9.6 %)
	SON	0.134	0.122(−9.0 %)	0.206(+53.7 %)	0.195(+45.6 %)
	Annual	0.569	0.526(−7.6 %)	0.813(+42.9 %)	0.779(+36.9 %)
BC	DJF	0.036	0.038(+5.6 %)	0.029(−19.4 %)	0.030(−16.7 %)
	MAM	0.045	0.045(0.0 %)	0.037(−17.8 %)	0.037(−17.8 %)
	JJA	0.024	0.021(−12.5 %)	0.016(−33.3 %)	0.015(−37.5 %)
	SON	0.028	0.028(0.0 %)	0.020(−28.6 %)	0.019(−32.1 %)
	Annual	0.133	0.132(−0.8 %)	0.102(−23.3 %)	0.101(−24.1 %)
OC	DJF	0.076	0.076(0.0 %)	0.054(−28.9 %)	0.057(−25.0 %)
	MAM	0.113	0.110(−2.7 %)	0.098(−13.3 %)	0.094(−16.8 %)
	JJA	0.056	0.046(−17.9 %)	0.045(−19.6 %)	0.035(−37.5 %)
	SON	0.053	0.050(−5.7 %)	0.035(−34.0 %)	0.032(−39.6 %)
	Annual	0.298	0.282(−5.4 %)	0.232(−22.1 %)	0.218(−26.8 %)
$PM_{2.5}$	DJF	1.004	1.090(+8.6 %)	1.208(+20.3 %)	1.195(+19.0 %)
	MAM	1.170	1.170(0.0 %)	1.384(+18.3 %)	1.370(+17.1 %)
	JJA	0.737	0.622(−15.6 %)	0.864(+17.2 %)	0.771(+4.6 %)
	SON	0.836	0.802(−4.1 %)	1.017(+21.7 %)	0.984(+17.7 %)
	Annual	3.747	3.681(−1.8 %)	4.473(+19.4 %)	4.320(+15.3 %)

[a] Seasonal and annual total fluxes averaged over 1999–2001.
[b] Year 2050 fluxes simulated with climate change alone.
[c] Year 2050 fluxes simulated with changes in anthropogenic emissions alone
[d] Year 2050 fluxes simulated with changes in both climate and anthropogenic emissions.

Table 5. Simulated transport of aerosols to or from southern China through the latitudinal plane along 20° N from 90 to 125° E. Positive (negative) values indicate northward (southward) transport. Numbers in the parentheses are percentage changes in absolute values of fluxes relative to the present-day values.

Species		2000[a] (Tg)	Transport to or from Southern China 2050[b] (Tg)	2050[c] (Tg)	2050[d] (Tg)
SO_4^{2-}	DJF	−0.066	−0.179(171.2 %)	0.061(192.4 %)	−0.053(19.7 %)
	MAM	0.099	0.106(7.1 %)	0.419(323.2 %)	0.407(311.1 %)
	JJA	0.002	0.002(0.0 %)	0.074(3600.0 %)	0.065(3150.0 %)
	SON	−0.163	−0.145(11.0 %)	−0.095(41.7 %)	−0.074(54.6 %)
	Annual	−0.128	−0.216(68.8 %)	0.459(458.6 %)	0.345(369.5 %)
NO_3^-	DJF	−0.012	−0.048(300.0 %)	−0.015(25.0 %)	−0.057(375.0 %)
	MAM	0.101	0.037(63.4 %)	0.159(57.5 %)	0.021(79.2 %)
	JJA	−0.099	−0.094(5.1 %)	−0.309(212.1 %)	−0.268(170.7 %)
	SON	−0.068	−0.055(19.1 %)	−0.067(1.5 %)	−0.054(20.6 %)
	Annual	−0.078	−0.16(105.1 %)	−0.232(197.4 %)	−0.358(359.0 %)
NH_4^+	DJF	−0.018	−0.055(205.6 %)	0.030(266.7 %)	−0.014(22.2 %)
	MAM	0.069	0.052(24.6 %)	0.214(210.1 %)	0.167(142.0 %)
	JJA	−0.025	−0.024(4.0 %)	−0.065(160.0 %)	−0.056(124.0 %)
	SON	−0.059	−0.048(18.6 %)	−0.040(32.2 %)	−0.029(50.8 %)
	Annual	−0.033	−0.075(127.3 %)	0.139(521.2 %)	0.068(306.1 %)
BC	DJF	0.009	−0.009(200.0 %)	0.018(100.0 %)	0.008(11.1 %)
	MAM	0.100	0.096(4.0 %)	0.119(+19.0 %)	0.115(15.0 %)
	JJA	0.004	0.006(50.0 %)	0.005(+25.0 %)	0.006(50.0 %)
	SON	−0.015	−0.011(26.7 %)	−0.003(+80.0 %)	−0.002(86.7 %)
	Annual	0.098	0.082(16.3 %)	0.139(+41.8 %)	0.127(29.6 %)
OC	DJF	0.098	0.047(52.0 %)	0.102(4.1 %)	0.066(32.7 %)
	MAM	0.584	0.557(4.6 %)	0.659(12.8 %)	0.633(8.4 %)
	JJA	0.021	0.026(23.8 %)	0.012(42.9 %)	0.014(33.3 %)
	SON	−0.016	−0.013(18.8 %)	−0.006(62.5 %)	−0.005(68.8 %)
	Annual	0.687	0.617(10.2 %)	0.767(11.6 %)	0.708(3.1 %)
$PM_{2.5}$	DJF	0.011	−0.243(2309.1 %)	0.195(1672.7 %)	−0.050(554.5 %)
	MAM	0.953	0.847(11.1 %)	1.571(64.8 %)	1.342(40.8 %)
	JJA	−0.096	−0.084(12.5 %)	−0.283(194.8 %)	−0.239(149.0 %)
	SON	−0.321	−0.272(15.3 %)	−0.210(34.6)	−0.163(49.2 %)
	Annual	0.547	0.248(54.7 %)	1.273(132.7 %)	0.890(62.7 %)

[a] Seasonal and annual total fluxes averaged over 1999–2001.
[b] Year 2050 fluxes simulated with climate change alone.
[c] Year 2050 fluxes simulated with changes in anthropogenic emissions alone.
[d] Year 2050 fluxes simulated with changes in both climate and anthropogenic emissions.

Title Page

Abstract | Introduction

Conclusions | References

Tables | Figures

◄ | ►

◄ | ►

Back | Close

Full Screen / Esc

Printer-friendly Version
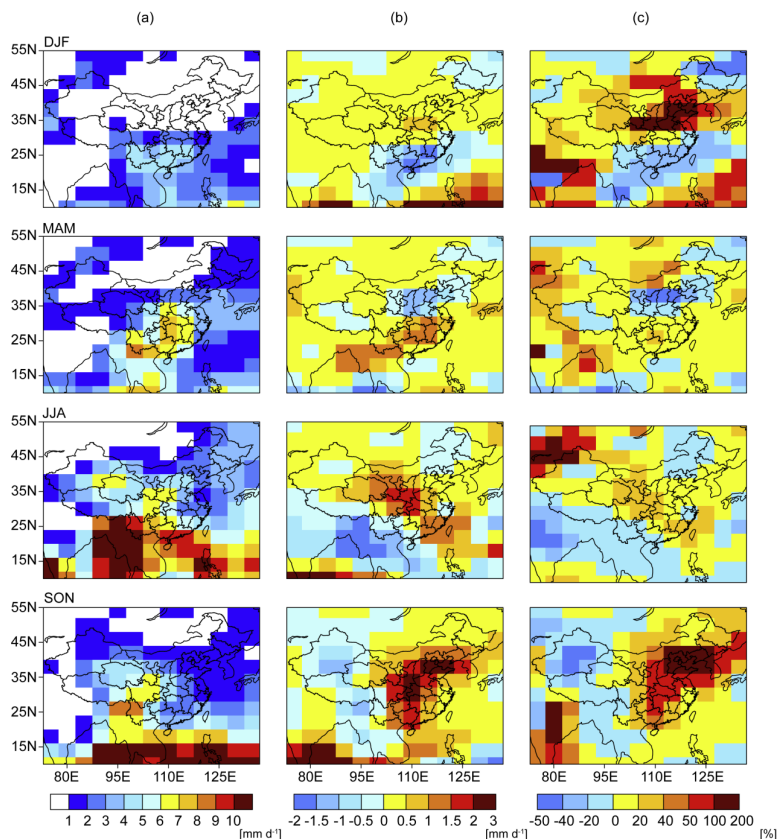
Interactive Discussion
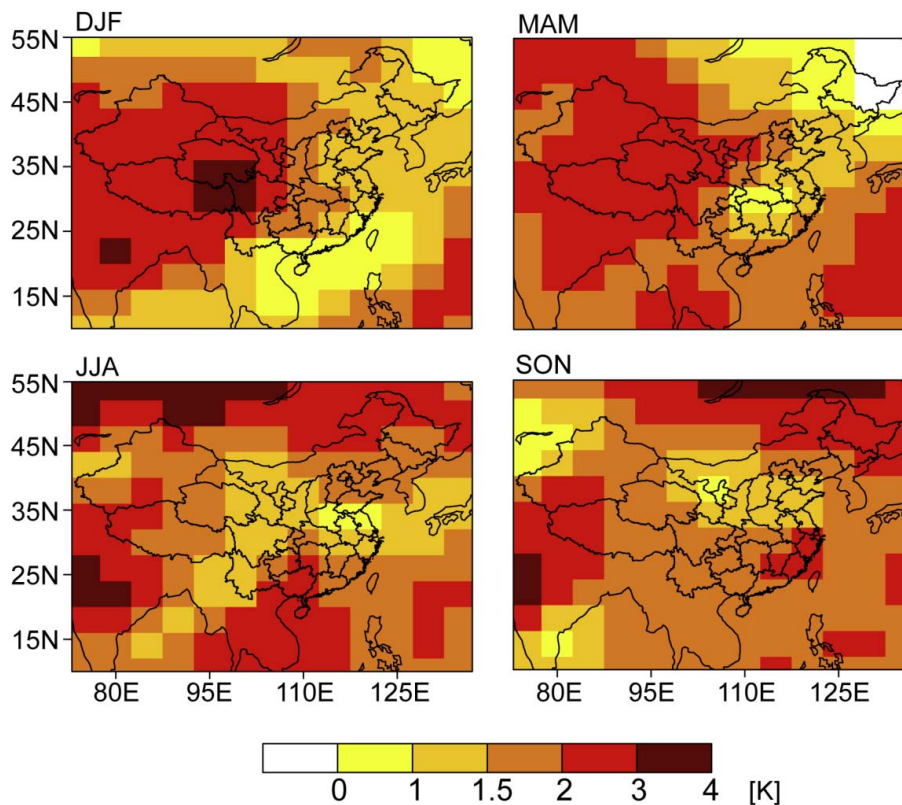
Fig. 1. Projected changes in surface air temperature (K) in China from the present day (1999–2001) to future (2049–2051) under the IPCC A1B scenario.
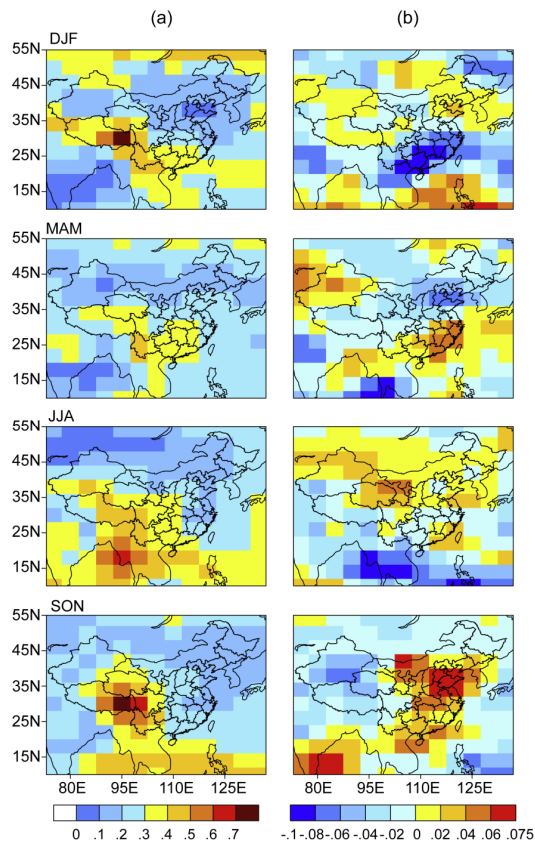
Fig. 2. (a) Simulated precipitation (mm day^{-1}) in China in present day; **(b)** projected changes in precipitation (mm day^{-1}) in China from the present day (1999–2001) to future (2049–2051) under the IPCC A1B scenario; **(c)** the percentage changes in precipitation relative to present day.

Title Page

Abstract | Introduction

Conclusions | References

Tables | Figures

|◄ | ►|

◄ | ►

Back | Close

Full Screen / Esc

Printer-friendly Version

Interactive Discussion

Fig. 3. (a) Simulated cloud fraction (unitless) in China in present day; **(b)** projected changes in cloud fraction in China from the present day (1999–2001) to future (2049–2051) under the IPCC A1B scenario.

Title Page

Abstract | Introduction

Conclusions | References

Tables | Figures

|◄ | ►|

◄ | ►

Back | Close

Full Screen / Esc

Printer-friendly Version

Interactive Discussion
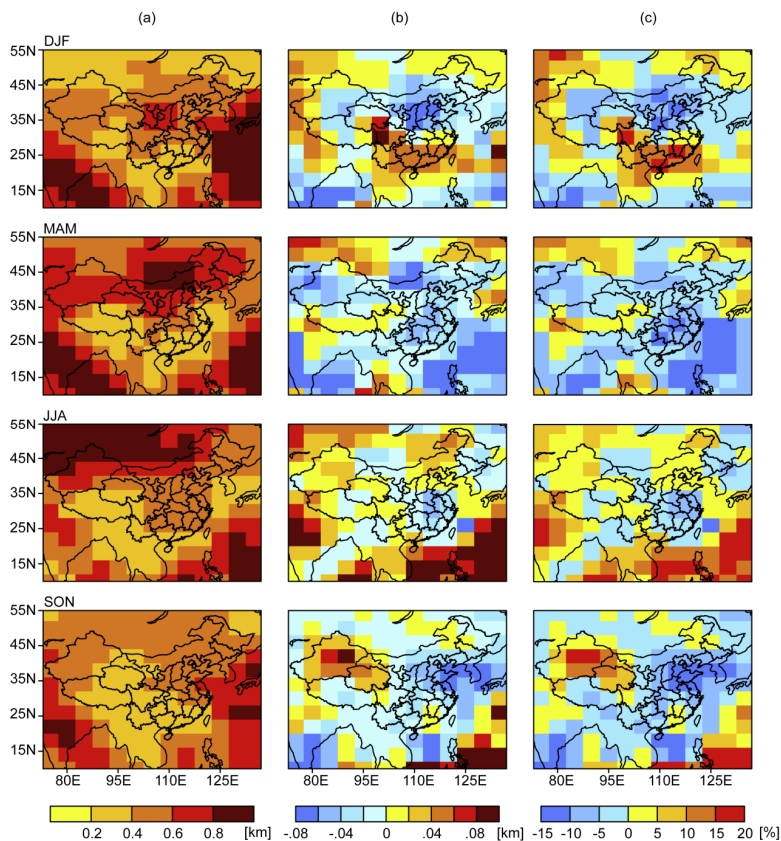
Fig. 4. (a) Simulated planetary boundary layer (PBL) depth (km) in China in present day; **(b)** projected changes in PBL depth (km) in China from the present day (1999–2001) to future (2049–2051) under the IPCC A1B scenario; **(c)** the percentage changes in PBL depth relative to present day.
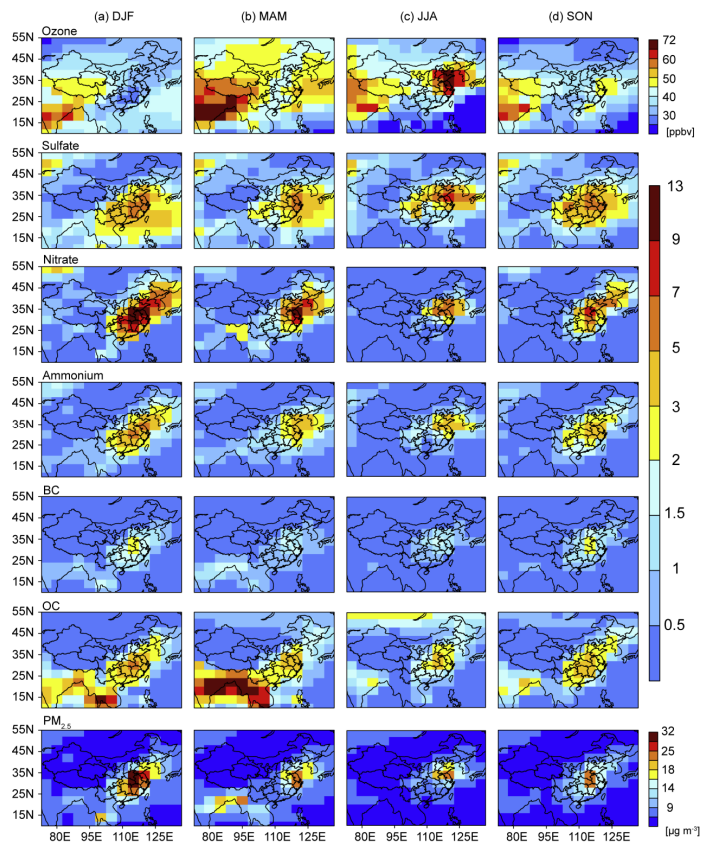
Fig. 5. Simulated present-day seasonal mean surface-layer concentrations of O_3, SO_4^{2-}, NO_3^-, NH_4^+, BC, OC, and $PM_{2.5}$ in China. Concentrations of O_3 are in ppbv and those of aerosols in $\mu g \, m^{-3}$.
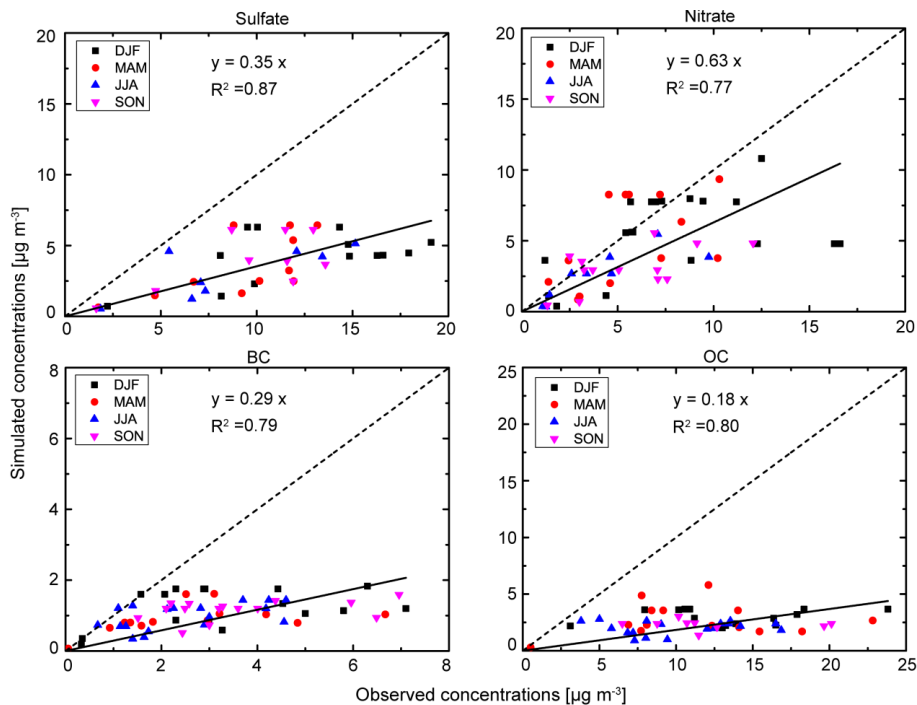
Fig. 6. Present-day predictions of sulfate, nitrate, BC, and OC aerosols compared to observations. Simulated values are seasonal averages for the 3-yr period 1999–2001. Also shown is the 1 : 1 line (dashed) and linear fit (solid line and equation). *R* is the correlation coefficient between simulated and measured concentrations.

Discussion Paper | Discussion Paper | Discussion Paper | Discussion Paper |

ACPD

13, 6501–6551, 2013

Projected 2000–2050 changes in aerosols in China

H. Jiang et al.

Title Page

Abstract | Introduction

Conclusions | References

Tables | Figures

|◀ | ▶|

◀ | ▶

Back | Close

Full Screen / Esc

Printer-friendly Version

Interactive Discussion
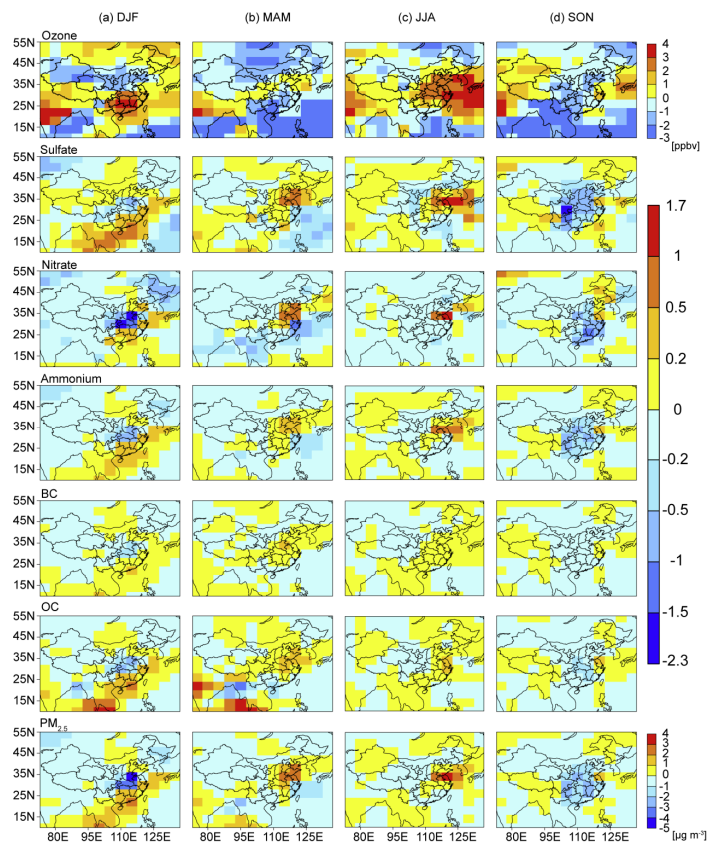
Fig. 7. Predicted changes in surface-layer concentrations of O_3 (ppbv) and aerosols ($\mu g\,m^{-3}$) due to changes in climate alone from the present day (1999–2001) to the future (2049–2051). Greenhouse gases follow the IPCC scenario A1B. Anthropogenic emissions are held at present-day values, but natural emissions may change in response to climate.
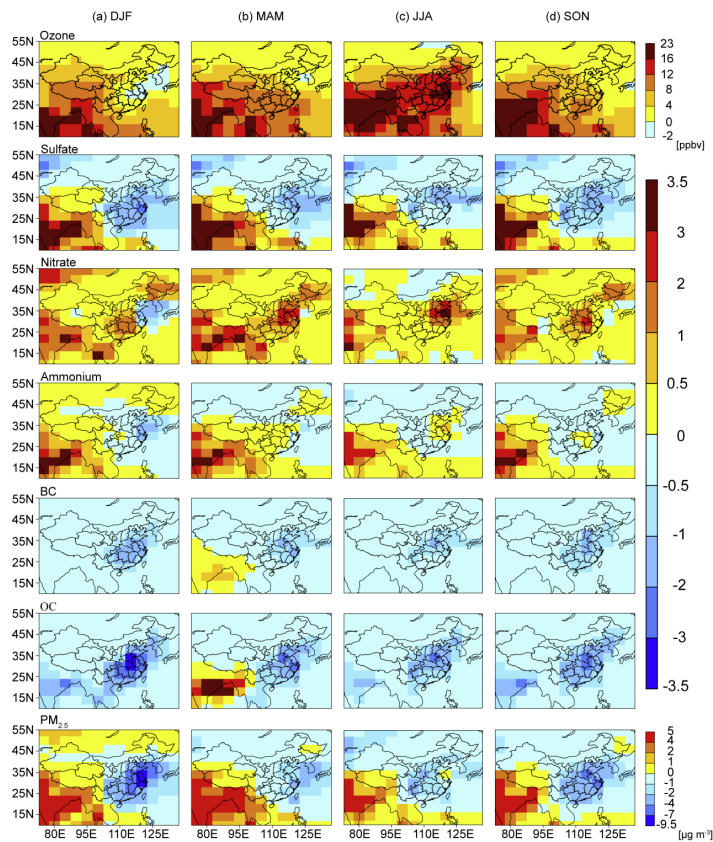
Fig. 8. Predicted changes in surface-layer concentrations of O$_3$ (ppbv) and aerosols (µg m^{-3}) due to changes in anthropogenic emissions alone from the present day (1999–2001) to the future (2049–2051).

Fig. 9. Predicted changes in surface-layer concentrations of O_3 (ppbv) and aerosols ($\mu g\,m^{-3}$) due to changes in both climate and anthropogenic emissions from the present day (1999–2001) to the future (2049–2051).

Title Page

Abstract | Introduction

Conclusions | References
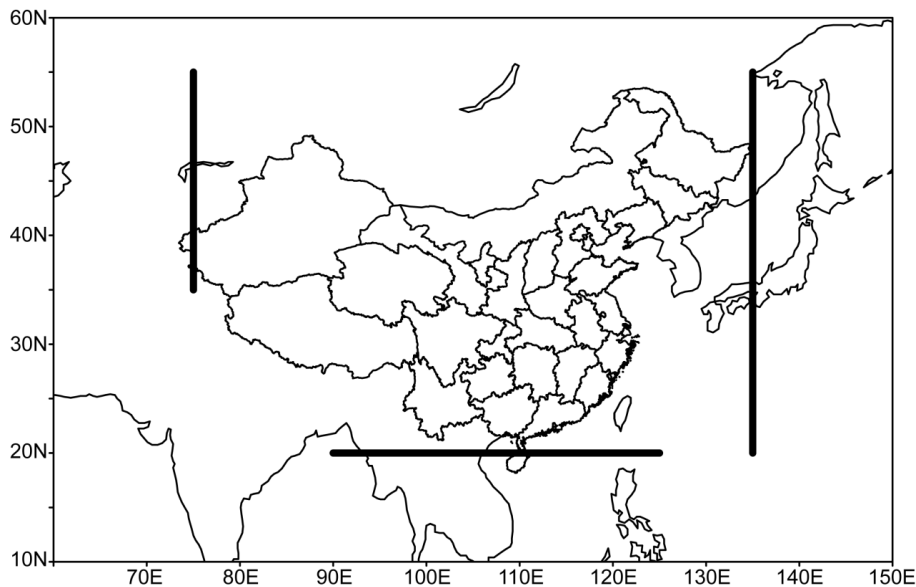
Tables | Figures

◀ | ▶|

◀ | ▶

Back | Close

Full Screen / Esc

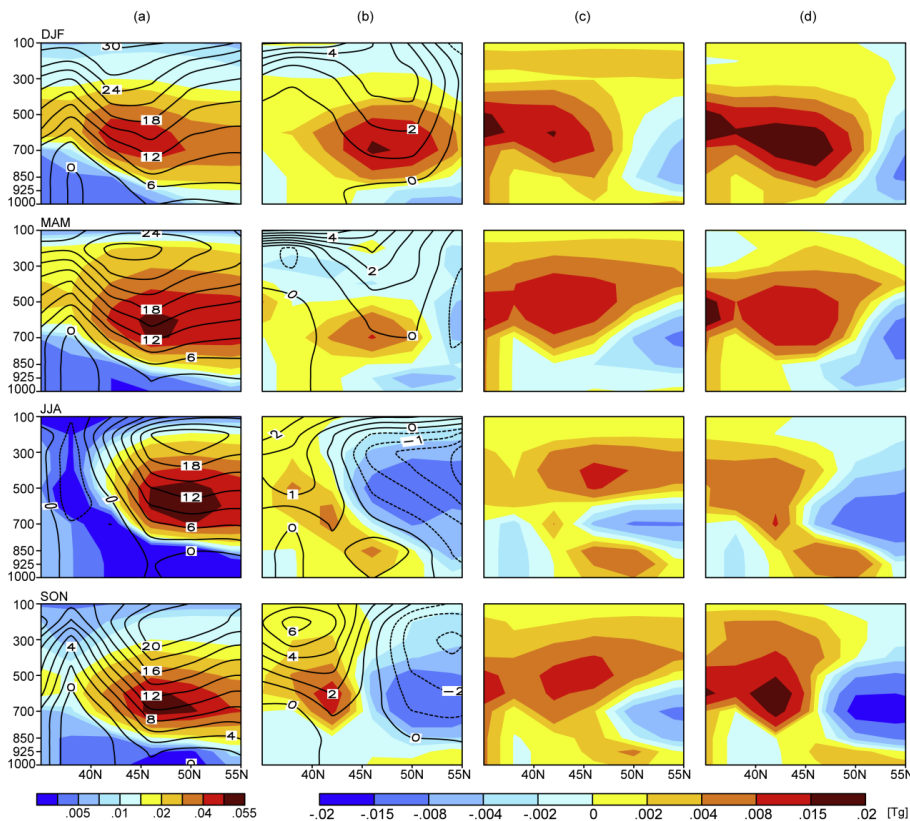Printer-friendly Version

Interactive Discussion

Fig. 10. The locations of the 3 vertical planes through which fluxes of transboundary aerosols are calculated: the meridional plane along 135° E from 20 to 55° N that captures the outflow from eastern China to the western Pacific, the meridional plane along 75° E from 35 to 55° N that captures the inflow from Europe and Central Asia to China, and the latitudinal plane along 20° N from 90 to 125° E to capture the transport to or from South Asia and Southeast Asia.

Title Page

Abstract | Introduction

Conclusions | References

Tables | Figures

◄ | ►

◄ | ►

Back | Close

Full Screen / Esc

Printer-friendly Version

Interactive Discussion
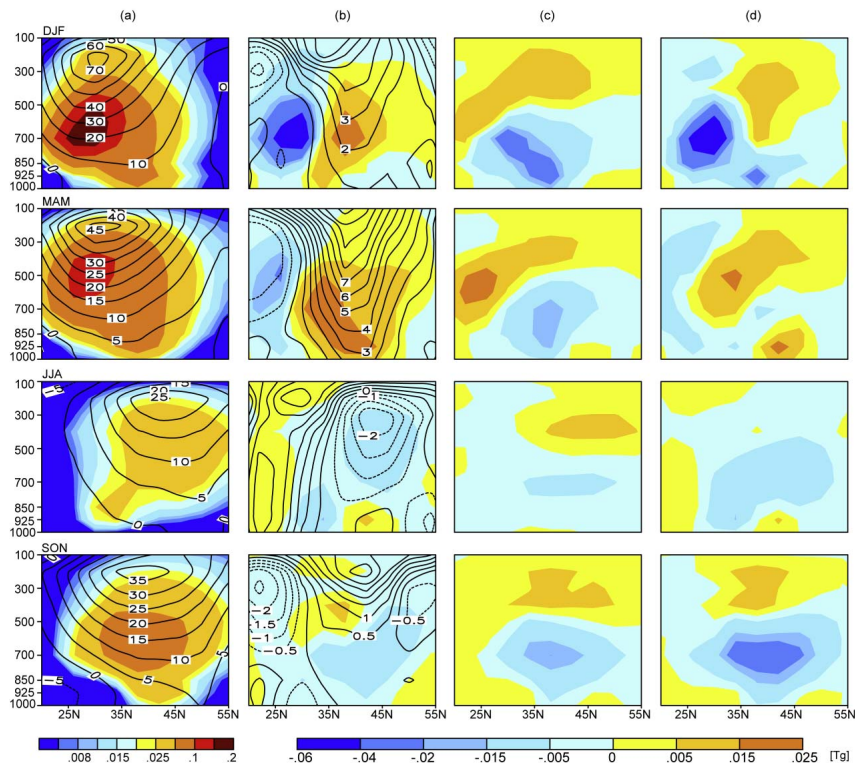
Fig. 11. (a) Simulated present-day mass fluxes of PM$_{2.5}$ and zonal winds; **(b)** projected changes in mass fluxes of PM$_{2.5}$ and zonal winds from the present day (1999–2001) to future (2049–2051) owing to climate change alone; **(c)** projected changes in mass fluxes of PM$_{2.5}$ from the present day to future owing to the changes in anthropogenic emissions alone; **(d)** projected changes in mass fluxes of PM$_{2.5}$ from the present day to future owing to the changes in both climate and anthropogenic emissions. Mass fluxes of PM$_{2.5}$ are shown by shades (units: Tg) and winds are represented by contours (units: m s^{-1}). Both mass fluxes and winds are those across the meridional plane along 135° E from 20 to 55° N.

Title Page

Abstract | Introduction

Conclusions | References

Tables | Figures

|◀ | ▶|

◀ | ▶

Back | Close

Full Screen / Esc

Printer-friendly Version

Interactive Discussion

ACPD

13, 6501–6551, 2013

Projected 2000–2050
changes in aerosols
in China

H. Jiang et al.

Fig. 12. Same as Fig. 11 but mass fluxes and winds are those through the meridional plane along 75° E from 35 to 55° N.
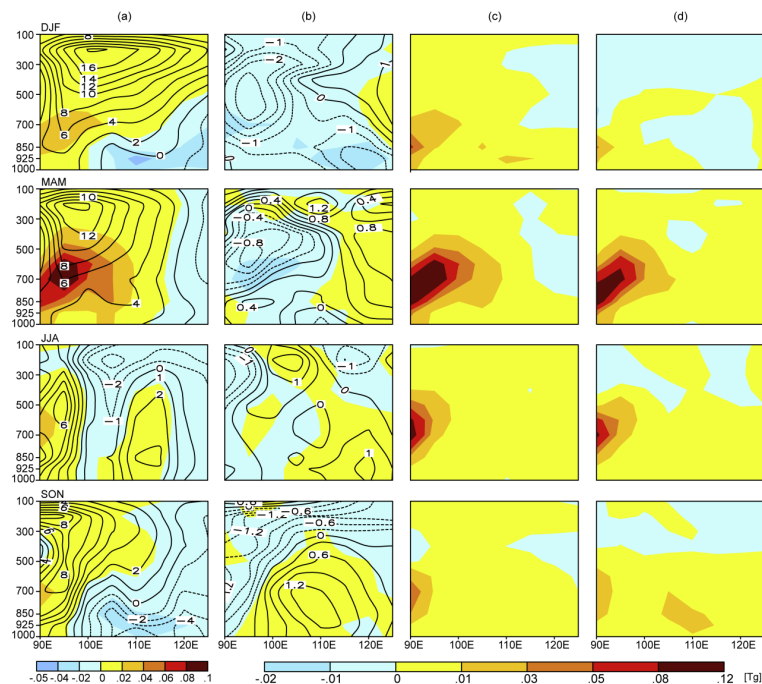
Fig. 13. **(a)** Simulated present-day mass fluxes of PM$_{2.5}$ and meridional winds; **(b)** projected changes in mass fluxes of PM$_{2.5}$ and meridional winds from the present day (1999–2001) to future (2049–2051) owing to climate change alone; **(c)** projected changes in mass fluxes of PM$_{2.5}$ from the present day to future owing to the changes in anthropogenic emissions alone; **(d)** projected changes in mass fluxes of PM$_{2.5}$ from the present day to future owing to the changes in both climate and anthropogenic emissions. Mass fluxes of PM$_{2.5}$ are shown by shades (units: Tg) and winds are represented by contours (units: m s^{-1}). Both mass fluxes and winds are those through latitudinal plane along 20° N from 90 to 125° E. Positive (negative) fluxes indicate northward (southward) transport.

Title Page

Abstract | Introduction

Conclusions | References

Tables | Figures

|◀ | ▶|

◀ | ▶

Back | Close

Full Screen / Esc

Printer-friendly Version

Interactive Discussion